JOURNAL OF GEOPHYSICAL RESEARCH, VOL. 105, NO. E8, PAGES 20,207–20,225, AUGUST 25, 2000

Photochemical modeling of CH_3 abundances in the outer solar system

Anthony Y. T. Lee and Yuk L. Yung

Division of Geological and Planetary Sciences, California Institute of Technology, Pasadena

Julianne Moses

Lunar and Planetary Institute, Houston, Texas

Abstract. Recent measurements of methyl radicals (CH_3) in the upper atmospheres of Saturn and Neptune by the Infrared Space Observatory (ISO) provide new constraints to photochemical models of hydrocarbon chemistry in the outer solar system. The derived column abundances of CH_3 on Saturn above 10 mbar and Neptune above the 0.2 mbar pressure level are $(2.5 - 6.0) \times 10^{13}$ cm^{-2} and $(0.7 - 2.8) \times 10^{13}$ cm^{-2}, respectively. We use the updated Caltech/Jet Propulsion Laboratory photochemical model, which incorporates hydrocarbon photochemistry, vertical molecular and bulk atmospheric eddy diffusion, and realistic radiative transfer modeling, to study the CH_3 abundances in the upper atmosphere of the giant planets and Titan. We identify the key reactions that control the concentrations of CH_3 in the model, such as the three-body recombination reaction, $CH_3 + CH_3 + M \rightarrow C_2H_6 + M$. We evaluate and extrapolate the three-body rate constant of this reaction to the low-temperature limit ($1.8 \times 10^{-16} T^{-3.75} e^{-300/T}$, $T < 300$ K) and compare methyl radical abundances in five atmospheres: Jupiter, Saturn, Uranus, Neptune, and Titan. The sensitivity of our models to the rate coefficients for the reactions $H + CH_3 + M \rightarrow CH_4 + M$, $H + C_2H_3 \rightarrow C_2H_2 + H_2$, $^1CH_2 + H_2 \rightarrow CH_3 + H$, and $H + C_2H_5 \rightarrow 2\ CH_3$, the branching ratios of CH_4 photolysis, vertical mixing in the five atmospheres, and Lyman α photon enhancement at the orbit of Neptune have all been tested. The results of our model CH_3 abundances for both Saturn (5.1×10^{13} cm^{-2}) and Neptune (2.2×10^{13} cm^{-2}) show good agreement with ISO Short Wavelength Spectrometer measurements. Using the same chemical reaction set, our calculations also successfully generate vertical profiles of stable hydrocarbons consistent with Voyager and ground-based measurements in these outer solar system atmospheres. Predictions of CH_3 column concentrations (for $p \leq 0.2$ mbar) in the atmospheres of Jupiter (3.3×10^{13} cm^{-2}), Uranus (2.5×10^{12} cm^{-2}), and Titan (1.9×10^{15} cm^{-2}) may be checked by future observations.

1. Introduction

Studies of photochemistry in the reducing atmospheres of the outer solar system were pioneered by *Strobel* [1973, 1975] and others. More recent contributions to our understanding of hydrocarbon photochemistry include the comprehensive works of *Gladstone et al.* [1996] for Jupiter, *Moses et al.* [2000a, b] for Saturn, *Summers and Strobel* [1989] for Uranus, *Romani et al.* [1993] and *Bishop et al.* [1998] for Neptune, and *Yung et al.* [1984], *Toublanc et al.* [1995], and *Lara et al.* [1996] for Titan. All of these modeling works consider a straightforward photochemical scheme initiated by methane (CH_4) photolysis followed by radical-radical and radical-molecule interactions that eventually lead to the synthesis of complex hydrocarbons. These models provide a satisfactory explanation for the observations of stable hydrocarbon molecules, such as CH_4, C_2H_2, C_2H_4, and C_2H_6, obtained from the extensive ground-based and spacecraft (Voyager) observations. However, a rigorous test of the theory of hydrocarbon photochemistry, and a systematic comparison between these models using a consistent set of photochemical reactions applied to all the atmospheres of the outer solar system, is still lacking.

Recent observations of hydrocarbon species by the Short Wavelength Spectrometer (SWS) on the Infrared Space Observatory (ISO) provide new insights into the hydrocarbon photochemistry in the atmospheres of the outer solar system. The first detection of methyl radicals (CH_3) in the outer solar system was made in the atmospheres of Saturn and Neptune by ISO [*Bézard et al.*, 1998, 1999]. CH_3 is one of the most important radicals in hydrocarbon photochemistry because it is a product of methane photolysis and plays an essential role in forming C_2H_6, the most abundant and stable C2 species. These observations pose a challenge to current photochemical models.

The CH_3 column densities deep in the stratosphere of Saturn obtained by ISO/SWS observations were first analyzed by *Bézard et al.* [1998] to be $(1.5 - 7.5) \times 10^{13}$ cm^{-2} above 0.2 mbar and were reanalyzed by *Moses et al.* [2000a] to be $(2.5 - 6.0) \times 10^{13}$ cm^{-2} above 10 mbar. The amount of CH_3 in the stratosphere of Neptune by ISO/SWS observations is

Paper number 1999JE001186.
0148-0227/00/1999JE001186$09.00

$(0.7 - 2.8) \times 10^{13}$ cm^{-2} above 0.2 mbar [*Bézard et al.*, 1999]. Current hydrocarbon photochemical models tend to overpredict the CH_3 column abundance value when using the traditionally adopted CH_3-CH_3 recombination rate constant from *Slagle et al.* [1988]. The observational value for Saturn is about a factor of 5 - 10 lower than the prediction of hydrocarbon photochemical models in which the *Slagle et al.* rate constant is used [e.g., *Bézard et al.*, 1998; *Atreya et al.*, 1998]. According to these researchers, the discrepancy could be attributed to one of two possibilities. Either the eddy diffusion coefficients on Saturn are ~ 100 times less than the standard values, or the self-reaction loss rate constant for CH_3 is about a factor of 10 higher than the value given by *Slagle et al.* [1988]. However, the first possibility is not convincing because decreasing the eddy diffusion coefficients by 2 orders of magnitude violates the Voyager measurements (Saturn: *Courtin et al.* [1984]) in the atmosphere of those giant planets, and there is no other reason to believe in an arbitrary reduction of vertical transport since the Voyager epoch. In fact, both *Bézard et al.* [1998] and *Moses et al.* [2000a] present current models in which the CH_3 abundance matches the ISO observations by assuming a higher CH_3 recombination rate constant. We will therefore reexamine the currently adopted recombination rate constants for methyl-methyl recombination at low temperature and provide quantitative results for CH_3 column abundances in the stratospheres of those planets.

Hydrocarbon photochemistry in the upper atmospheres of the outer solar system is initiated by photolysis of methane. Primary products of CH_4 photodissociation are CH, $^1CH_2$, $^3CH_2$, and CH_3 radicals. Although the branching ratios of the various possible CH_4 photolysis pathways at the hydrogen Lyman α line are not well determined [*Smith and Raulin*, 1999; *Romani*, 1996; *Moses et al.*, 2000a], a detailed analysis of chemical reactions following primary photodissociation shows that a large portion of $^1CH_2$ radicals readily convert CH_3 in the presence of H_2. The main paths forming CH_3 in the altitudes above 10^{-4} mbar in Jupiter or in Saturn are as follows:

$$CH_4 + h\nu \rightarrow CH_3 + H$$

or

$$CH_4 + h\nu \rightarrow {}^1CH_2 + H_2$$

$$CH_4 + h\nu \rightarrow {}^1CH_2 + 2H$$

followed by

$$^1CH_2 + H_2 \rightarrow CH_3 + H.$$

These pathways dominate the production of CH_3 radicals in the upper stratospheres of the outer solar system (see detailed discussion in section 2). In the middle and lower stratospheres, where less production of CH_3 radicals by photolysis is occurring, the formation of CH_3 by the reaction $H + C_2H_5 \rightarrow 2CH_3$ becomes important. A detailed discussion of the hydrocarbon chemistry can be found in a recent book by *Yung and DeMore* [1999]. Figure 1 shows the major pathways for producing and removing CH_3 radicals in the stratospheres of the outer solar system.

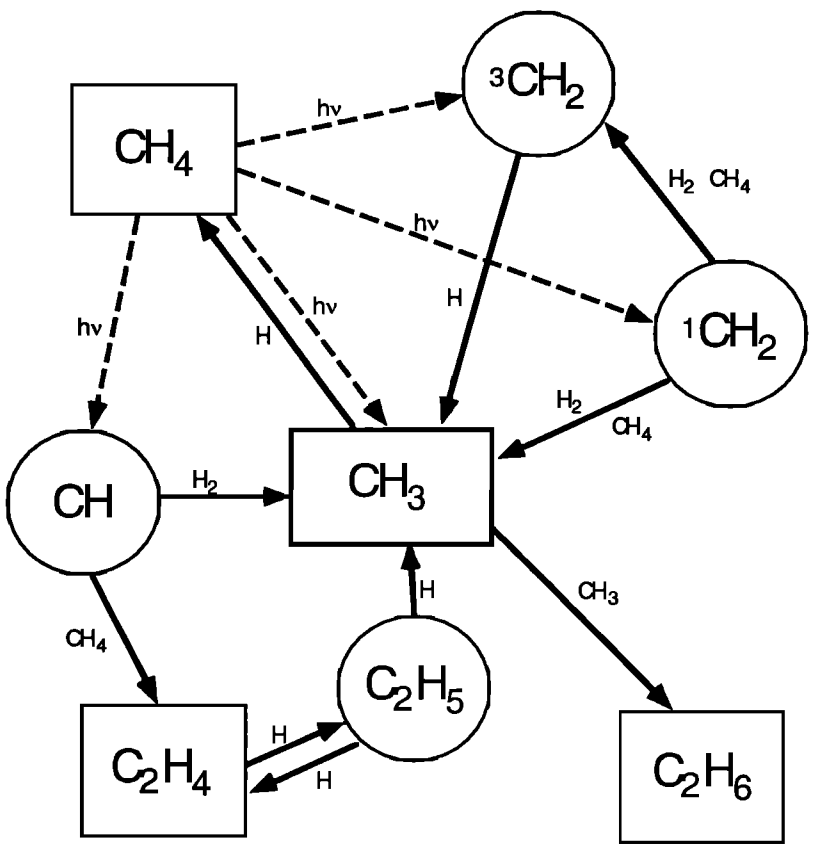

Figure 1. Major reaction pathways for methyl radical (CH_3) photochemistry.

Table 1. High-Pressure Two-Body (k_∞) and Low-Pressure Three-Body (k_0) Rate Constants of Recombination Reaction $CH_3 + CH_3 + M \rightarrow C_2H_6 + M$

	High-Pressure Rate Constant k_∞	Low-Pressure Rate Constant k_0
Slagle[a]	$1.5\times10^{-7}\,T^{-1.18}\,e^{-329/T}$	$8.76\times10^{-7}\,T^{-7.03}\,e^{-1390/T}$
MacPherson[b]	$4.09\times10^{-11}\,e^{137/T}$	$6.0\times10^{-29}\,e^{1680/T}$
Modified Slagle[c,d]	6.0×10^{-11}	$1.8\times10^{-16}\,T^{-3.75}\,e^{-300/T}$

[a]The formulas are valid between 296 and 906 K.

[b]The formulas are valid between 296 and 577 K; k_∞ is from *MacPherson et al.* [1985] while k_0 is from *MacPherson et al.* [1983]

[c]The formula for k_0 is valid only at $T < 300$ K. For $T > 300$ K, the Slagle formula is applied.

[d] The broadening factor of low-pressure rate constant k_0 is as same as the value of Slagle, $F_{cent} = 0.381\,e^{-T/73.2} + 0.619\,e^{-T/1180}$.

In hydrogen-rich environments like the upper atmospheres of the outer solar system, a large portion of CH_3 radicals recycles back immediately to CH_4 by the reaction

$$H + CH_3 + M \rightarrow CH_4 + M. \quad (1)$$

The high-pressure limit rate constant k_∞ and low-pressure limit rate constant k_0 of (1) used in our models will be discussed in the next section.

One of the most important reactions for the CH_3 radical is the self-recombination reaction to form the stable ethane (C_2H_6) molecule; it is also one of the major sinks of CH_3 radicals in the upper stratosphere:

$$CH_3 + CH_3 + M \rightarrow C_2H_6 + M. \quad (2)$$

This three-body recombination reaction has been intensively studied and measured in the laboratory [*Hole and Mulcahy*, 1969; *Van den Bergh*, 1976; *MacPherson et al.*, 1983, 1985; *Slagle et al.*, 1988; *Du et al.*, 1996] and theoretical studies [*Wagner and Wardlaw*, 1988; *Forst*, 1991; *Robertson et al.*, 1995; *Klippenstein and Harding*, 1999]. Two widely used empirical rate constant functions from *Slagle et al.* [1988] and *MacPherson et al.* [1983, 1985] are shown in Table 1. However, most of the kinetic rate coefficients for this reaction were measured at room temperature or higher. The extrapolation to low temperatures below 200 K, typical of stratospheric temperatures in the outer solar system, by current theoretical techniques is highly uncertain. *Allen* [1989] has pointed out the importance of the temperature dependence of the CH_3 recombination reaction and the possible influence for chemical models of planetary atmospheres. We will evaluate the extrapolation of the three-body rate constant of (2) to temperatures lower than 300 K in section 2. Along with these two reactions, the rate constants for some related reactions will also be discussed. Table 2 lists these reactions.

For the purpose of comparison, we use a one-dimensional diurnally averaged photochemical model to test the impact of the rate constant of (2) on the abundances of CH_3 radicals in different atmospheres of the outer solar system. Similar photochemical models have been developed for four planets and one satellite: Jupiter, Saturn, Uranus, Neptune, and Titan. Identical lists of photochemical reactions, cross sections, and rate constants were used for all of the planets, but other parameters such as the physical properties of the planet and its atmosphere (e.g., radius, mass, heliocentric distance, temperature-pressure profile, eddy diffusion coefficient profile, and radiation flux) were specific to each planet. All physical data for model atmospheres are taken from Voyager and ground-based measurements [*Yung and DeMore*, 1999]. By adopting the modified rate constant of (2) at low temperatures deduced in this work, our models for the atmospheres of Saturn and Neptune show reasonable agreement with the CH_3 abundances observed by ISO/SWS, and our models also show reasonable agreement with the Voyager observations for stable hydrocarbon molecules. Therefore we have confidence that our models provide reliable estimates of CH_3 concentrations in the atmospheres of Jupiter, Uranus, and Titan. These predictions may be checked by future observations.

2. Models and Chemical Kinetics

We developed one-dimensional photochemical models of the upper atmospheres of Jupiter, Saturn, Uranus, Neptune, and Titan on the basis of updated generic Caltech/Jet Propulsion Laboratory photochemical model [e.g., *Gladstone et al.*, 1996]. Comprehensive studies applying this model to hydrocarbon photochemistry in the upper atmosphere of Titan, Jupiter, and Saturn have been presented by *Yung et al.* [1984], *Gladstone et al.* [1996], and *Moses et al.* [2000a, b], respectively. Because similar photochemical processes operate in the five atmospheres of the outer solar system, we adopt the same set of photochemical cross sections and chemical reactions in all of our models. The physical properties of the atmospheres, such as pressure, temperature, density, eddy diffusion coefficients, or basic planetary parameters like the distance from the Sun and gravity, are the principal differences between the planetary atmospheres. We use the most complete and recently updated set of hydrocarbon photochemical reactions taken from *Moses et al.* [2000a], except for some key reactions, which are discussed in this article. Readers can refer to Tables II and III in their paper for detailed discussion and Table 2 of this paper for the key chemical reactions whose rate coefficients we have modified.

Table 2. Rate Constants of Key Reactions Adopted in Our Models

Reaction	Rate Constant	Reference
$H + CH_3 + M \rightarrow CH_4 + M$	$k_0 = 2.3\times10^{-17}\,T^{-4.03}\,e^{-1366/T}$ ($T > 300$ K)	1
	$k_0 = 1.4\times10^{-19}\,T^{-3.75}\,e^{-300/T}$ ($T < 300$ K)	see text
$H + C_2H_3 \rightarrow C_2H_2 + H_2$	7.50×10^{-11}	2; see text
$H + C_2H_5 \rightarrow 2\,CH_3$	6.0×10^{-11}	3
$^1CH_2 + H_2 \rightarrow CH_3 + H$	7.00×10^{-11} ($T < 150$ K)	see text
	9.24×10^{-11} ($T > 150$ K)	
$2CH_3 + M \rightarrow C_2H_6 + M$	$k_0 = 1.8\times10^{-6}\,T^{-3.75}\,e^{-300/T}$ $k_\infty = 6.0\times10^{-11}$ ($T < 300$ K)	see text

The units of rate constants in this table are $cm^3\ s^{-1}$ (two-body reaction) and $cm^6\ s^{-1}$ (three-body reaction). References: 1, *Moses et al.*, 2000a.; 2, *Monks et al.*, 1995; 3, *Baulch et al.*, 1992.

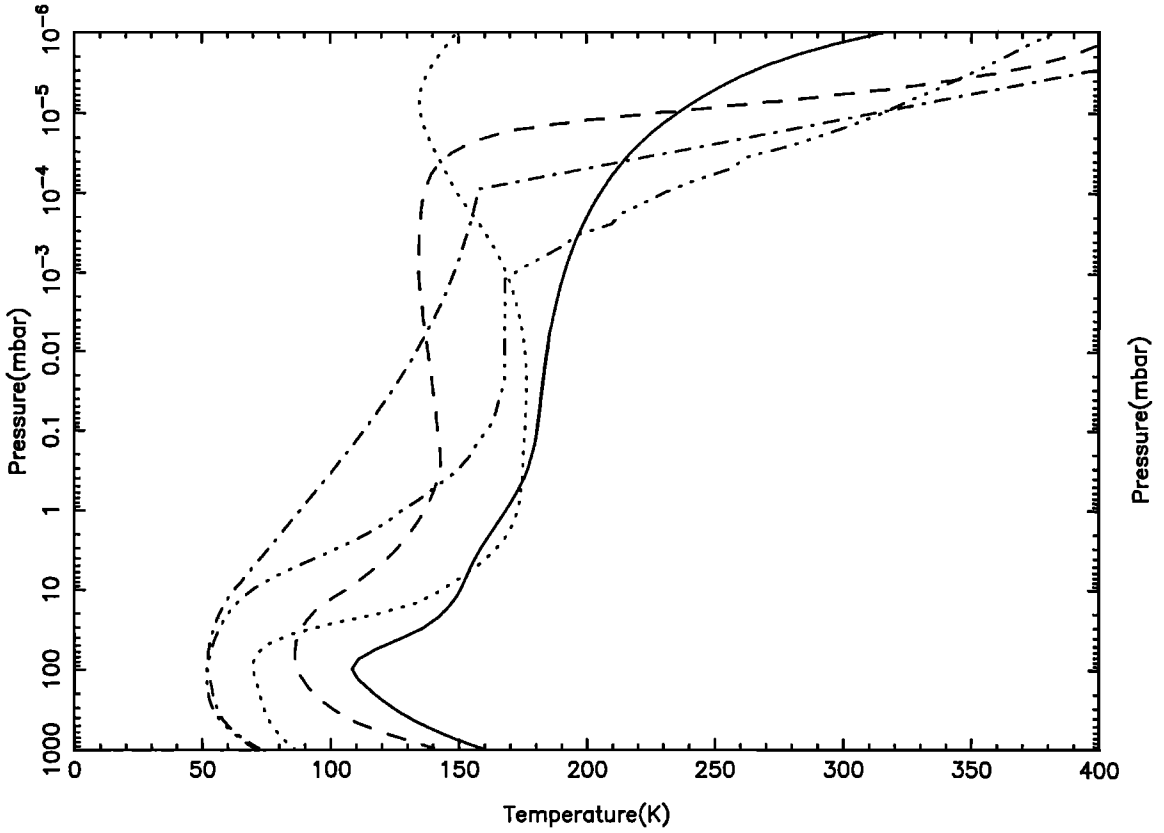

Figure 2. Temperature profiles used for the model atmospheres: Jupiter (solid), Saturn (dashed), Uranus (dash-dot), Neptune (dash-dot-dot-dot), and Titan (dotted).

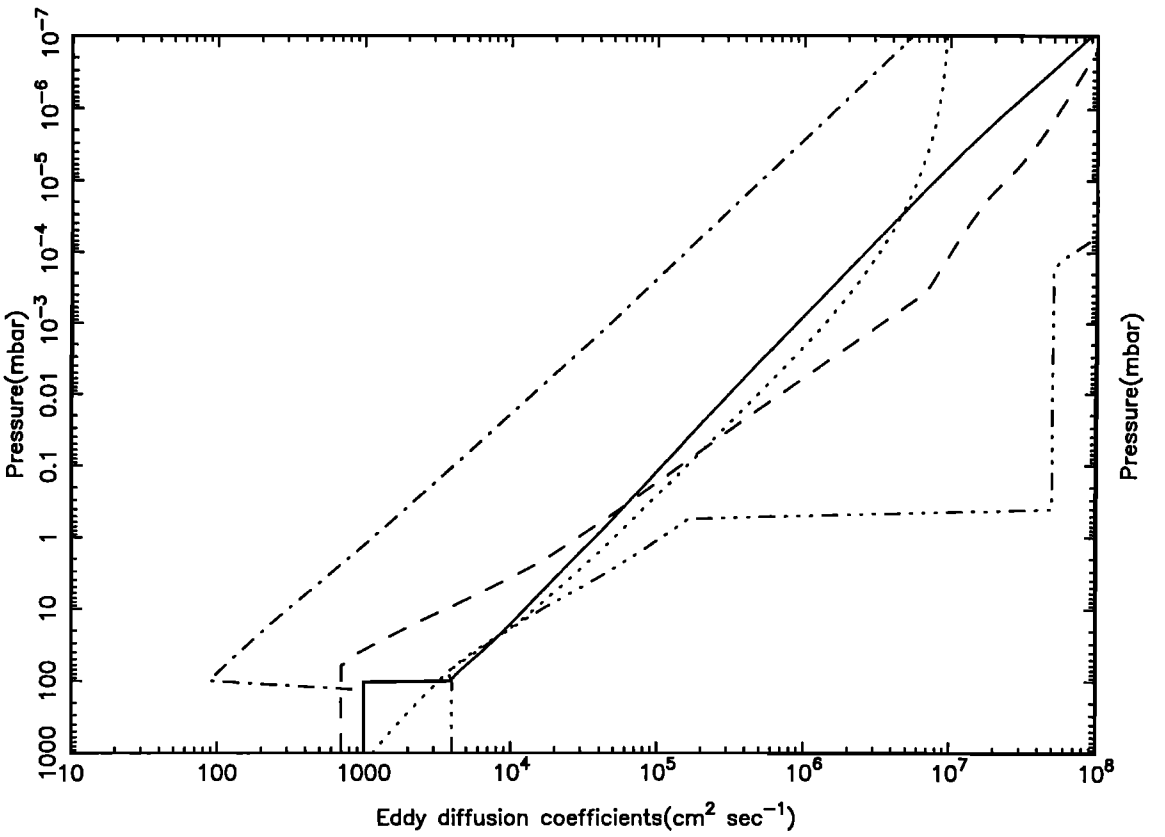

Figure 3. Eddy diffusion profiles used for the model atmospheres of Jupiter, Saturn, Uranus, Neptune, and Titan. The lines denote the same planets as in Figure 2.

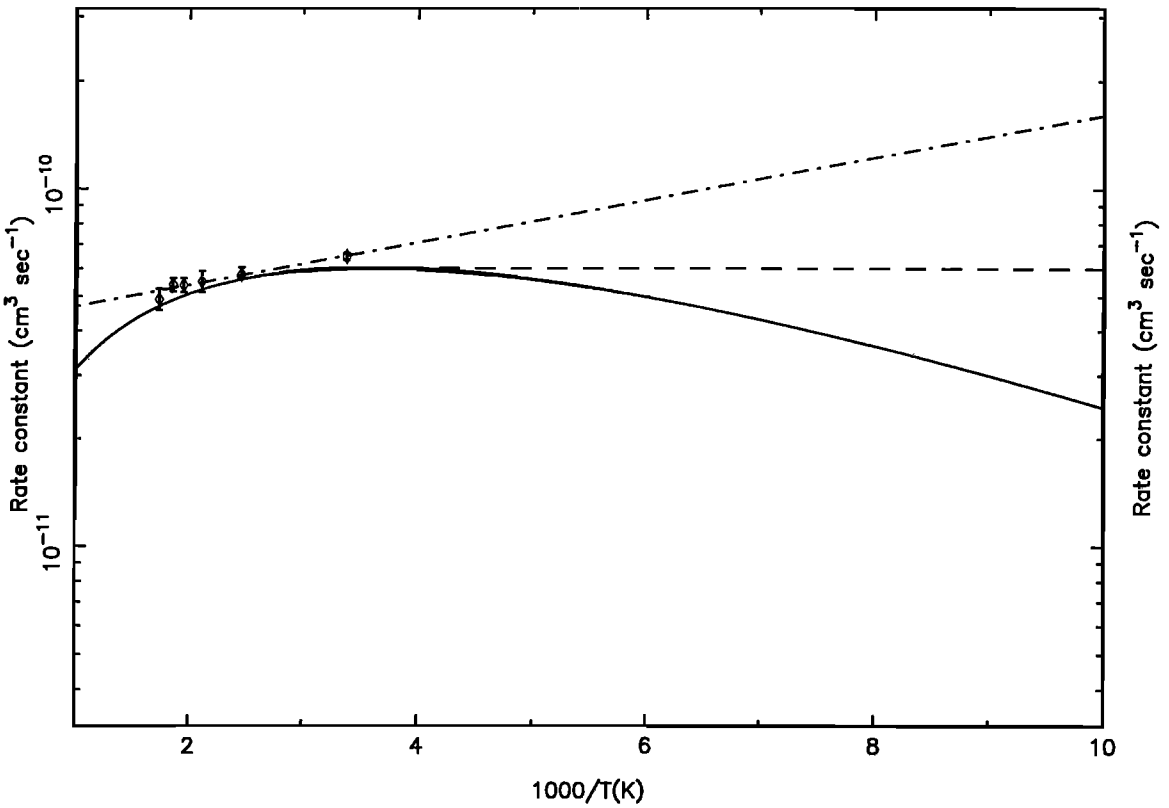

Figure 4. High-pressure (two-body) rate constant of $CH_3 + CH_3 \rightarrow C_2H_6$ reaction at temperatures from 100 to 1000K. The solid line, dashed line, and dash-dotted line denote the rate constant formulas derived from *Slagle et al.* [1988], Modified Slagle (this work), and *MacPherson et al.* [1983, 1985], respectively. The points with error bars from 296 to 577 K are laboratory results by MacPherson *et al.* [1983, 1985].

Model atmospheres of the planets are assumed to be hydrostatic, and the pressure-temperature profiles are determined principally from Voyager measurements. In this work, we take the atmospheric parameters of Titan, Jupiter, and Saturn from previous models by *Yung et al.* [1984], *Gladstone et al.* [1996], and *Moses et al.* [2000a], respectively. The thermal structure and vertical mixing in the upper atmosphere of Uranus used in our model are taken from *Herbert et al.* [1987] and *Summers and Strobel* [1989]. The temperature profile for Neptune is taken from *Lindal* [1992] and *Broadfoot et al.* [1989]. The eddy diffusion coefficient of the stratosphere of Neptune is critical for hydrocarbon modeling. We use the eddy-mixing profile suggested by *Romani et al.* [1993], with $K \approx 5 \times 10^7$ cm^2 s^{-1} for $0.5 > p > 10^{-4}$ mbar, because it provides a reasonable fit to the lower limit of the C_2H_6 mixing ratio from the Voyager Infrared Radiometer Interferometer and Spectrometer (IRIS) observations (1×10^{-6}) in the lower stratosphere. Figure 2 presents the pressure-temperature profiles in the upper atmospheres of Jupiter, Saturn, Titan, Uranus, and Neptune used in our models; Figure 3 shows the vertical eddy diffusion coefficient profiles in the upper atmospheres of those models.

Bézard et al. [1998, 1999] pointed out the importance of the rate constant of the recombination reaction (2) at lower temperatures ($T < 200$ K) in determining the CH_3 abundance on the outer planets. The pressure and temperature regimes where significant CH_4 photodissociation and (2) occur are $p \approx 10^{-3}$–10^{-4} mbar and $T \approx 120$ to 160 K in the atmospheres of Saturn or Neptune. However, the rate constant of (2) is uncertain since no reliable measurements of the rate constant have been made at any temperature below 200 K in laboratory studies. Also, all of the theoretical studies [*Wagner and Wardlaw*, 1988; *Forst*, 1991; *Robertson et al.*, 1995; *Klippenstein and Harding*, 1999] of the rate constant function via temperature are unconfirmed under 296 K. Empirical extrapolations of the low-pressure rate constant k_0 and high-pressure rate constant k_∞ by *Slagle et al.* [1988], and *MacPherson et al.* [1983, 1985], are shown in Table 1.

Figures 4 and 5 give the two-body and three-body rate constants, respectively, calculated from 100 to 1000 K, using the formulas of *Slagle et al.* [1988] (solid line) and *MacPherson et al.* [1983, 1985] (dash-dotted line) extrapolated to temperatures outside the range in which the formulas were designed. Figures 4 and 5 also include the experimental kinetics data in the two-body (high-pressure) and three-body (low-pressure) limit measured by *MacPherson et al.* [1983, 1985]. Both functions by Slagle et al. and *MacPherson et al.* [1983, 1985] are consistent with experimental values within their error bars above 300 K, but they significantly deviate from each other at low temperatures. *MacPherson et al.*'s [1983, 1985] formulas increase sharply at low temperatures because of the positive exponents, which are adopted for matching the increasing trend of experimental values above 300 K. In contrast, the formula of Slagle et al. decreases when we move to the low-temperature regime, which is opposite to the experimental trend at higher temperatures. We believe that the Slagle et al. formulas are

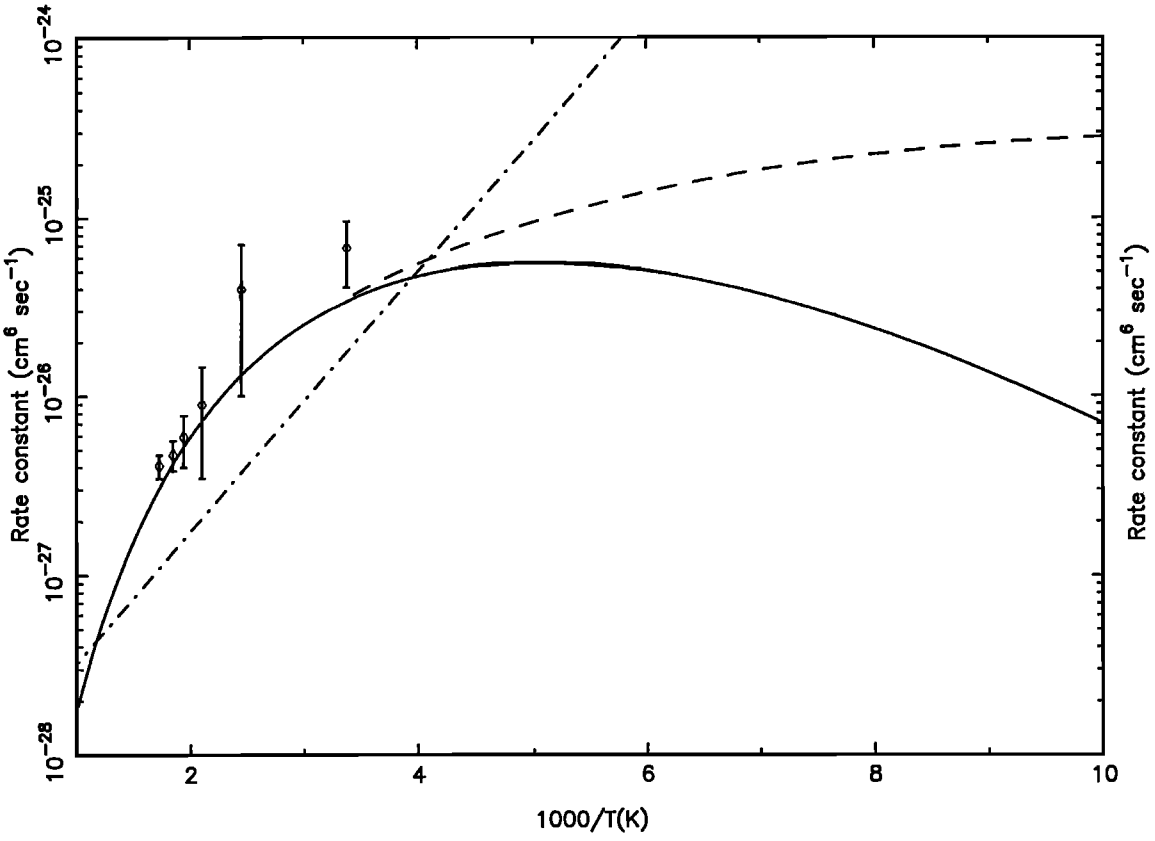

Figure 5. Same as Figure 4, but for the low-pressure (three-body) rate constant of $CH_3 + CH_3 + M \rightarrow C_2H_6 + M$.

correct only within their temperature range (296 K < T < 906 K) and cannot provide reasonable extrapolation at low temperatures (100 K < T < 200 K). In particular, the low-pressure rate constant k_0 tends to increase as temperature decreases owing to the possible longer lifetime of the intermediate activated complex formed in three-body collisions. The drastic decrease predicted by Slagle et al.'s formula is thus unreasonable. On the other hand, a very rapid increase of rate constant when T < 150 K for *MacPherson et al.*'s [1983] extrapolation at low temperatures is also hard to justify, because of the bulk slower motion of the reactants. There are 2 orders of magnitude difference between these formulas at 150 K, which is the typical temperature of the stratospheres of the outer solar system.

Our approach is based on an alternative estimate of the rate constant for (2). Heuristic reasons [*Troe*, 1977a, b; *Laufer et al.*, 1983] are briefly described as follows, along with preliminary estimates. For the high-pressure limit $CH_3 + CH_3 \rightarrow C_2H_6$, the rate constant k_∞ tends to increase as temperature is reduced to 200 K because of the shift in the position of the transition state to larger C-C bonding distance. This effect may continue as temperature approaches 100 K. On the other hand, the collision frequency goes as the square root of temperature, which tends to counteract the effect of the changing transition state. These two effects may contribute comparable but opposite corrections to the low-temperature reaction rate. Therefore we propose a constant $k_\infty = 6.0 \pm 3.0 \times 10^{-11}$ cm^3 s^{-1} for T less than 300 K. This value and the error bar were suggested by *Baulch et al.* [1992] and are also consistent with all laboratory measurement values below 1000 K. At temperatures higher than 300 K, we adopt *Slagle et al*'s [1988] two-body rate constant formula, obtaining

$$k_\infty = 1.5 \times 10^{-11} T^{-1.18} e^{137/T} \text{ cm}^3 \text{ s}^{-1} \quad T > 300 \text{ K}$$
$$k_\infty = 6.0 \pm 3.0 \times 10^{-11} \text{ cm}^3 \text{ s}^{-1} \quad T < 300 \text{ K} \tag{3}$$

For the three-body rate constant k_0, we expect an increase of k_0 as the temperature decreases owing to the longer lifetime of the intermediate activated complex as the internal thermal energy decreases in the low-temperature regime [*Laufer et al.*, 1983]. Slower motion and a smaller rate of collisions counteract this effect, as mentioned previously. These effects suggest a gradual increase of k_0 at low temperature. We can also notice this increasing trend for the measured rate constants at 500, 400, and 300 K, by a factor of 2 - 3, from Figure 5. At 300 K the *Slagle et al.* [1988] formula gives k_0 (300 K) = 3.3×10^{-26} cm^6 s^{-1}; thus reasonable estimates for k_0 at low temperatures might be k_0 (200 K) ~ 1.0×10^{-25} cm^6 s^{-1} and k_0 (100 K) ~ 3.0×10^{-25} cm^6 s^{-1}. By a smooth connection with Slagle et al.'s function at T > 300 K, we propose a low-pressure rate constant:

$$k_0 = 8.77 \times 10^{-7} T^{-7.03} e^{-1390/T} \text{ cm}^6 \text{ s}^{-1} \quad T > 300 \text{ K}$$
$$k_0 = 1.8 \times 10^{-6} T^{-3.75} e^{-300/T} \text{ cm}^6 \text{ s}^{-1} \quad T < 300 \text{ K} \tag{4}$$

Fitting the combination of the estimated values at 100, 200, and 300 K by using the Arrhenius expression derives this "modified Slagle's" formula. The dashed lines in both Figures 4 and 5 show the two-body and three-body "modified Slagle's" rate constants, respectively. The pressure

Table 3. Some Important Physical Properties in Our Models

	Jupiter	Saturn	Uranus	Neptune	Titan
Distance, AU	5.2	9.6	19.2	30.1	9.6
Gravity, cm s^{-2}	2325	1032	869	1100	135
Pressure, mbar	1.5×10^{-3}	5.9×10^{-5}	7.9×10^{-2}	2.4×10^{-4}	1.0×10^{-3}
Temperature,[a] K	191	139	116	209	169
Eddy coefficient, [a]cm^2 s^{-1}	7.5×10^{5}	1.2×10^{7}	4.7×10^{3}	5.0×10^{7}	1.3×10^{6}
Density,[a] cm^{-3}	5.6×10^{13}	3.1×10^{12}	5.0×10^{15}	8.2×10^{12}	4.6×10^{13}
Scale height,[a] km	29.3	55.3	45.3	71.4	54.0
CH_4 mixing, ratio,[a] ppmv	82.0	180.0	1.8	140.0	20,000
Dominant gas	H_2	H_2	H_2	H_2	N_2

The physical properties are given at the pressure level of the maximum CH_3 mixing ratio (i.e., where the most significant CH_3 photochemical reactions occur) in the atmospheres of Jupiter, Saturn, Uranus, and Neptune. In the case of Titan, we present the atmospheric data at the 10^{-3} mbar level because the maximum CH_3 mixing ratio is at and above the upper boundary level of our model.

[a]The values at the pressure level of the maximum CH_3 mixing ratio.

-broadening parameter F_{cent} for our estimated k_0 is assumed to be the same as Slagle's value: $F_{cent} = 0.381\ e^{-T/73.2} + 0.619\ e^{-T/1180}$. The bath gas for estimating the low-pressure rate constant is H_2, which is the dominant gas component in the atmospheres of Jupiter, Saturn, Uranus, and Neptune. The only exception is in the atmosphere of Titan, which is 98% N_2 (Table 3). Theoretically, H_2 is not as efficient as N_2 in deactivating the energized $C_2H_6^*$ molecule, so that three-body rate constants in H_2 bath gas may be slower than in N_2 bath gas. The three-body rate constants, especially for CH_3 recombination reaction and CH_3 recycling to CH_4 reaction, could be higher for Titan. However, we have tested the sensitivity of the model by increasing k_0 for $2CH_3 + M \rightarrow C_2H_6 + M$ and $H + CH_3 + M \rightarrow CH_4 + M$ by a factor of 1.5 for Titan. The result of the test run shows only small changes (< 10%), so that we may ignore the effect of different bath gases. The reason is that the above two reactions compete for CH_3 radicals. Hence, to first order, the efficiencies of the bath gases cancel. We must emphasize that these results are preliminary estimates. We expect to refine them with the application of the RRKM theory.

Moses et al. [2000a] evaluate the rate constant of (1) ($H + CH_3 + M \rightarrow CH_4 + M$) on the basis of actual rate measurements of *Brouard et al.* [1989] to derive the temperature-dependent low- and high-pressure limiting formulas for their Saturn model. The expression ((R95) in Table III in their paper) fits the 300 – 600 K data of *Brouard et al.* [1989] reasonably well. However, since the extrapolation to colder temperatures is uncertain, they assume constant rate constants below 300 K to avoid an unphysical turnover in the rates at low temperatures. We notice the similarity between (1) and (2), and would expect a gradual increase of k_0 of (1) when moving to the low temperatures. The following expression replaces the constant low-pressure limiting rate constant (2.5×10^{-29} cm^6 s^{-1}) at $T < 300$ K:

$$k_0 = 1.4\times10^{-19}\ T^{-3.75}\ e^{-300/T} \qquad T < 300\ \text{K} \qquad (5)$$

At 150 K this formula yields a low-pressure limiting rate constant value between the value estimated by *Moses et al.* [2000a] and the corresponding rate constant shown in Table 4 of *Gladstone et al.* [1996]. At temperatures above ~300 K we use the *Moses et al.* [2000a] expression.

Preliminary results showed stratospheric C_2H_2 abundances on Neptune that were lower than observations, so we reexamined the chemical production and destruction mechanisms of C_2H_2. The C_2H_2 abundance in the lower stratosphere ($0.1 - 5\times10^{-3}$ mbar) of Neptune is maintained by the two-body reaction $H + C_2H_3 \rightarrow C_2H_2 + H_2$. We expect that the rate constants used in previous models (6.0×10^{-12} cm^3 s^{-1} for *Gladstone et al.* [1996, (R85)]; 2.0×10^{-11} cm^3 s^{-1} for *Moses et al.* [2000a, (R100)]) could be underestimates. The direct experimental measurement of vinyl radicals reacting with hydrogen atoms by *Heinemann et al.* [1986] shows the rate constant 4.98×10^{-11} cm^3 s^{-1} at 293 K. *Monks et al.* [1995] have also determined the total rate constants of $H + C_2H_3 \rightarrow$ Products to be $(1.0\pm0.3)\times10^{-10}$ cm^3 s^{-1} at T = 213 and 298 K by laboratory experiments. Two major channels of vinyl radical reactions with a hydrogen atom, the three-body reaction (a) $H + C_2H_3 + M \rightarrow C_2H_4 + M$ and the two-body reaction (b) $H + C_2H_3 \rightarrow C_2H_2 + H_2$, have been considered. The fractional product yields Γ derived by Monks et al. show that pathway b dominates at low temperatures (i.e., $\Gamma_b(298\ K) = 0.67\pm0.18$ and $\Gamma_b(213\ K) = 0.76\pm0.16$). Considering all of these experimental facts, we adopt a reasonable rate constant value (7.5×10^{-11} cm^3 s^{-1}) for $H + C_2H_3 \rightarrow C_2H_2 + H_2$ to ensure that pathway b dominates. This value along with that for channel a producing C_2H_4, does not exceed the error bar of the total reaction rate coefficient for the reaction of vinyl radicals and H, $(1.0\pm0.3)\times10^{-10}$ cm^3 s^{-1}.

The photolysis of CH_4 at Lyman α (121.6 nm) is the starting point for producing complex hydrocarbon molecules in the upper region of these outer solar system atmospheres. Four kinds of radicals, CH_3, $^1CH_2$, $^3CH_2$, and CH, have been considered as possible fragments from the breaking of methane molecules by solar UV radiation. Different radicals lead to various routes and hydrocarbon products. Therefore the branching ratio of CH_4 photolysis may be important to determine product distributions between stable C2 hydrocarbons like C_2H_2 and C_2H_6. Unfortunately, the branching ratios of CH_4 at Lyman α are not well determined owing to the high reactivity of some of the photolysis products and to other experimental difficulties. In this work we adopt the branching ratios suggested by *Slanger and Black* [1982], which were used in the Jupiter hydrocarbon model by *Gladstone et al.* [1996]. The direct production of CH_3 by photolysis of CH_4 is negligible, and the primary channels for $^1CH_2$, $^3CH_2$, and CH are 47, 45, and 8%, respectively. However, *Moses et al.* [2000a] used the photodissociation channels by *Mordaunt et al.* [1993], *Ashfold et al.* [1992], and *Heck et al.* [1996] and other previous laboratory data. According to our sensitivity tests, these two sets of branching ratios lead to only minor differences for C2 hydrocarbon abundances on Jupiter, Saturn and Uranus that are within the errors of the observations. On the other hand, using different CH_4 photolysis channels would seriously affect C2 hydrocarbon mixing ratios on Neptune that could be

Table 4. Column Densities of CH_3 Radicals Above the Tropopause Region for Different Cases

	Slagle	MacPherson	Modified Slagle
Jupiter	4.5	1.5	3.3
Saturn	8.3	1.6	5.1
Titan	336	38.3	191
Uranus	0.37	0.18	0.25
Neptune	3.0	1.4	2.2

The column density values are in 10^{13} cm^{-2} and were measured at above 100 mbar pressure level.

distinguished by the Voyager IRIS observations. We will discuss the results in the sensitivity test section.

Since the C_2H_6/C_2H_2 ratios in the models seem to be affected by the primary radical yields following CH_4 photodissociation, the interradical exchange reactions could be important along with radical-molecule reactions. In our preliminary Neptune model we found that the C_2H_2 abundance in the lower stratosphere is sensitive to the interradical exchange reaction, $^1CH_2 + H_2 \rightarrow CH_3 + H$. The rate constant of the reaction $^1CH_2 + H_2 \rightarrow CH_3 + H$ may be overestimated in the previous planetary hydrocarbon models. *Gladstone et al.* [1996] and *Moses et al.* [2000a] use the value of 9.24×10^{-11} cm^3 s^{-1}, which was taken from absolute rate constants measured by Langford *et al.* [1983]. However, Langford et al. measured only the collisional removal rate of $^1CH_2$ radical with hydrogen molecule at 295 K. The experiment does not guarantee the dissociation of the H_2 molecule and the production of the CH_3 radical after collision. The earlier experimental rate constant of the same reaction by *Pilling and Robertson* [1977] is smaller than 9.24×10^{-11} cm^3 s^{-1}. Other similar reactions used in our model, $^1CH_2 + H_2 \rightarrow {}^3CH_2 + H_2$ ($k = 1.26 \times 10^{-11}$ cm^3 s^{-1}), $^1CH_2 + CH_4 \rightarrow {}^3CH_2 + CH_4$ ($k = 1.20 \times 10^{-11}$ cm^3 s^{-1}), and $^1CH_2 + CH_4 \rightarrow 2\ CH_3$ ($k = 5.9 \times 10^{-11}$ cm^3 s^{-1}), are not as fast. Therefore we estimate the rate constant of $^1CH_2 + H_2 \rightarrow CH_3 + H$ to be 7.0×10^{-11} cm^3 s^{-1} for $T < 150$ K, which is ~ 2/3 of the value determined by *Langford et al.* [1983] (see Table 2) at low temperatures. The actual value needs to be confirmed by laboratory experiments and theoretical studies.

We also change the $H + C_2H_5 \rightarrow 2\ CH_3$ reaction rate to $k = 6.0 \times 10^{-11}$ cm^3 s^{-1}, which was suggested by *Baulch et al.* [1992] other than by *Sillesen et al.* [1993]. All hydrocarbon chemical reactions that are different from Table III of *Moses et al.*'s [2000a] Saturn paper are summarized in Table 2.

This paper will focus on the consequences of using different CH_3 recombination rate constant expressions. In addition to the rate constant for (2), we will carry out a systematic testing of the sensitivity of CH_3 to all key reactions in the model, especially for Neptune. Also, the sensitivity to the temperature variation in the crucial pressure region $p \approx 10^{-3}$–10^{-4} mbar and to the vertical eddy diffusion coefficients on Saturn and Neptune will be tested. The validation of the photochemical model is extremely important for its application to atmospheric evolution. Eventually, the uncertainties in key rate coefficients will have to be resolved in laboratory studies. The modeling and sensitivity studies will help to focus the kinetics community on the critical issues.

3. Model Results

We calculated the CH_3 abundances by using our hydrocarbon photochemical models for five atmospheres. Some important physical properties and characteristics of the atmospheres at the pressure level where the CH_3 mixing ratio is a maximum (i.e., where the most significant CH_3 photochemical reactions occur) are presented in Table 3. For comparison, we carried out modeling studies using the three versions of rate constants for (2), discussed in the previous section. These cases are hereafter referred to as "Slagle," "MacPherson," and "Modified Slagle." The resulting CH_3 column densities are summarized in Table 4.

The column abundance values in Table 4 are total column densities of CH_3 above the lower stratosphere. The results for Saturn and Neptune can be compared to the ISO/SWS measurements. In Saturn the "Slagle" case yielded a value of 8.3×10^{13} cm^{-2}, about a factor of 1.5 higher than the observed value, $(2.5 - 6.0) \times 10^{13}$ cm^{-2}, deduced by *Moses et al.* [2000a] above the 10 mbar level. The excess of methyl radicals results from the low rate coefficient of *Slagle et al.*'s [1988] three-body formula for (2), as was first pointed out by *Bézard et al.* [1998, 1999]. There is obviously too little methyl radical loss via $CH_3 + CH_3 + M \rightarrow C_2H_6 + M$. On the other hand, the model value for the CH_3 column density obtained using "MacPherson" (1.6×10^{13} cm^{-2}) is less than the ISO observation. The value of "Modified Slagle" (5.1×10^{13} cm^{-2}) is in good agreement with the ISO/SWS measurement.

For the Neptune model, in comparison with the observational value $(0.7 - 2.8) \times 10^{13}$ cm^{-2} deduced by *Bézard et al.* [1999] above the 0.2 mbar level, both the "MacPherson" (1.4×10^{13} cm^{-2}) and "Modified Slagle" (2.2×10^{13} cm^{-2}) cases fit the ISO/SWS data within the uncertainty range. The "Slagle" value (3.0×10^{13} cm^{-2}) obviously fails to fit the observational range because of the slow rate of CH_3 loss from methyl-methyl recombination at the low temperatures of Neptune's stratosphere [cf. *Bézard et al.*, 1999]. The proposed "Modified Slagle" models for both Saturn and Neptune are in good agreement with ISO observations. However, the "MacPherson" rate constant formula also fits the CH_3 observations in Neptune. By considering both Saturn and Neptune cases, and the fact that the "MacPherson" formula gives unrealistic high rates at low temperatures, we therefore conclude that our modified expression for the CH_3 recombination rate provides the best fit to ISO observations among these candidates.

We may notice from Table 4 the low CH_3 column abundance in the upper stratosphere of Uranus and the high CH_3 column abundance in Titan. Lower values on Uranus than on other planets are due in large part to its smaller eddy mixing profile, as shown in Figure 3. This effect may be seen from the comparative studies for varying the bulk eddy diffusion coefficient in Saturn and Neptune in Table 5. On the other hand, the more stagnant atmosphere in Uranus confines methane to lower altitudes. In fact, according to our model and others [e.g., *Summers and Strobel*, 1989; *Herbert et al.*, 1987], the eddy diffusion coefficient profile in the stratosphere of Uranus is at least 2 orders of magnitude less than the eddy profiles in Jupiter and Saturn.

The unusually high total abundance of CH_3 radicals in the upper atmosphere of Titan is due to the low concentration of H atoms, resulting in very low probability for recycling CH_3 back to CH_4 via (1). Future observations of these atmospheres should provide tests for our model predictions.

Table 5. CH_3 Column Abundances in the Upper Atmospheres of Saturn and Neptune above 10 mbar for Saturn and 0.2 mbar for Neptune

CH_3 Column Abundances, cm^{-2}	Saturn	Neptune
ISO/SWS	$(2.5 - 6.0) \times 10^{13}$	$(0.7 - 2.8) \times 10^{13}$
Best fit model [a]	5.1×10^{13}	2.2×10^{13}
$T(z) + 10$ K [b]	5.4×10^{13}	2.4×10^{13}
$T(z) - 10$ K [c]	5.0×10^{13}	2.1×10^{13}
Bulk eddy × 2 [d]	8.5×10^{13}	2.6×10^{13}
Bulk eddy / 2 [e]	3.6×10^{13}	1.7×10^{13}

The CH_3 column abundance values were derived from sensitivity test models compared with the "best fit" model, which uses the reaction rate constants listed in Table 2.

[a]The "best fit" model denotes our current photochemical model using the modified Slagle rate constant of CH_3 recombination reaction, and the rate constant list in Table 2.

[b]Best fit model + increasing temperature by 10 K at all altitudes.

[c]Best fit model + decreasing temperature by 10 K at all altitudes.

[d]Best fit model + bulk atmospheric eddy diffusion coefficient times 2 at all altitudes.

[e]Best fit model + bulk atmospheric eddy diffusion coefficient divided by 2 at all altitudes.

Our models should provide results consistent with hydrocarbon observations, especially the Voyager data, in the atmospheres of the outer solar system. Figures 6 - 10 present the vertical profiles of the major hydrocarbon species in our models of Jupiter, Saturn, Uranus, Neptune, and Titan, respectively. The C_2H_2 and C_2H_6 measurements by Voyager are shown as pressure level ranges and error bars. The CH_3 recombination reaction rate constant used in all of those models is the "Modified Slagle" case. For the purpose of comparison, we have chosen the most abundant and long-lived disequilibrium hydrocarbon molecules, C_2H_2, C_2H_4, and C_2H_6, to be shown with the CH_3 radical in each plot. Most of these stable hydrocarbon profiles are in agreement with previous models and observations of the giant planets and Titan (e.g., Jupiter: *Gladstone et al.* [1996]; Saturn: *Moses et al.* [2000a, b] and *Lindal et al.* [1985]; Titan: *Yung et al.* [1984]; Uranus: *Summers and Strobel* [1989] and *Bishop et al.* [1990]; Neptune: *Romani et al.* [1993] and *Kostiuk et al.* [1992]).

For Jupiter, as shown in Figure 6, the C_2H_2 and C_2H_6 mixing ratio profiles compare reasonably well with the ground and satellite observations, including the Voyager IRIS measurement in the North Equatorial Belt (NEB) region (at a latitude of 10°N) with $f(C_2H_2) = (0.7 - 2.3) \times 10^{-8}$ from 1 to 60 mbar and $f(C_2H_6) = (0.8 - 3.0) \times 10^{-6}$ from 3 to 60 mbar (W. Maguire et al., private communication, 1993). The recent ground-based observations at midinfrared wavelengths by *Sada et al.* [1998] with $f(C_2H_2) = (1.8 - 2.8) \times 10^{-8}$ at 8 mbar and $f(C_2H_6) = (2.6 - 5.8) \times 10^{-6}$ at 5 mbar also show good

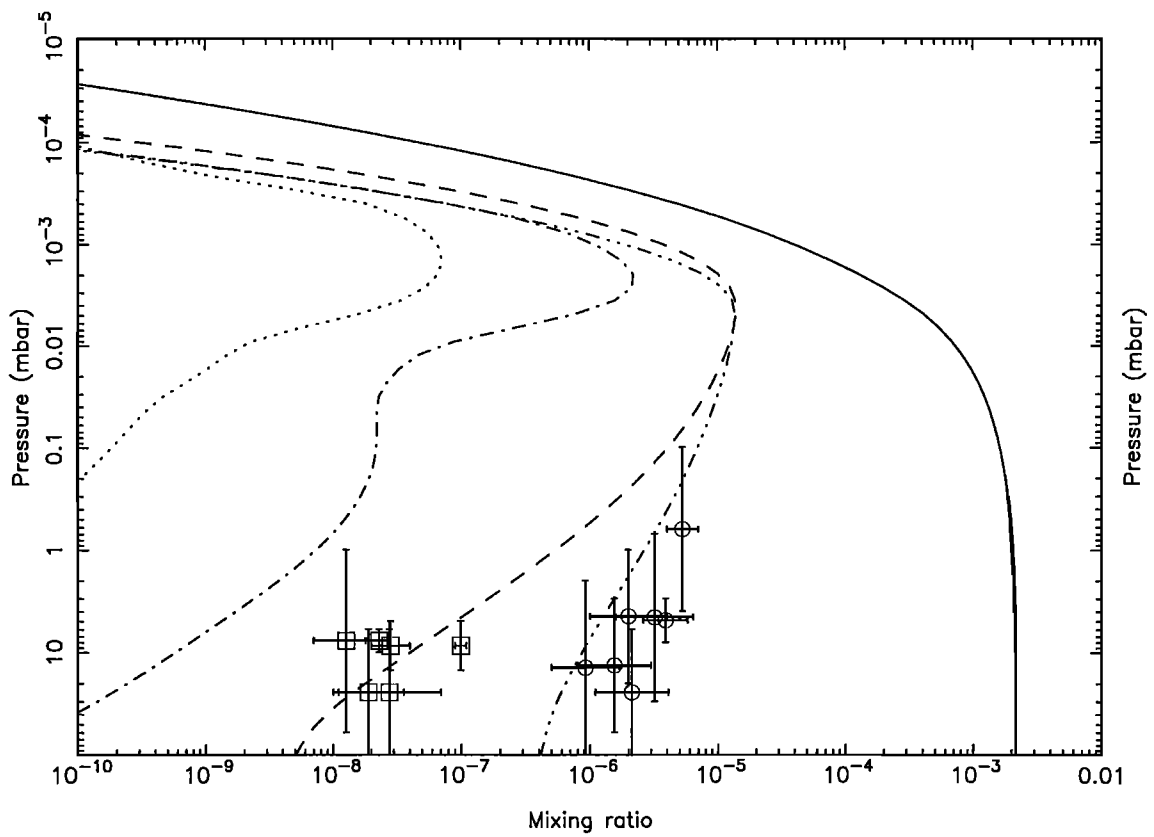

Figure 6. Model mixing ratios for hydrocarbons on Jupiter: CH_4 (solid), C_2H_2 (dashed), C_2H_4 (dash-dot), C_2H_6 (dash-dot-dot-dot), and CH_3 (dotted). This case was run by adopting the "Modified Slagle" rate constant for $CH_3 + CH_3 + M \rightarrow C_2H_6 + M$ reaction at low temperatures. Voyager IRIS and ground-based observations: C_2H_2 (open square) and C_2H_6 (open circle).

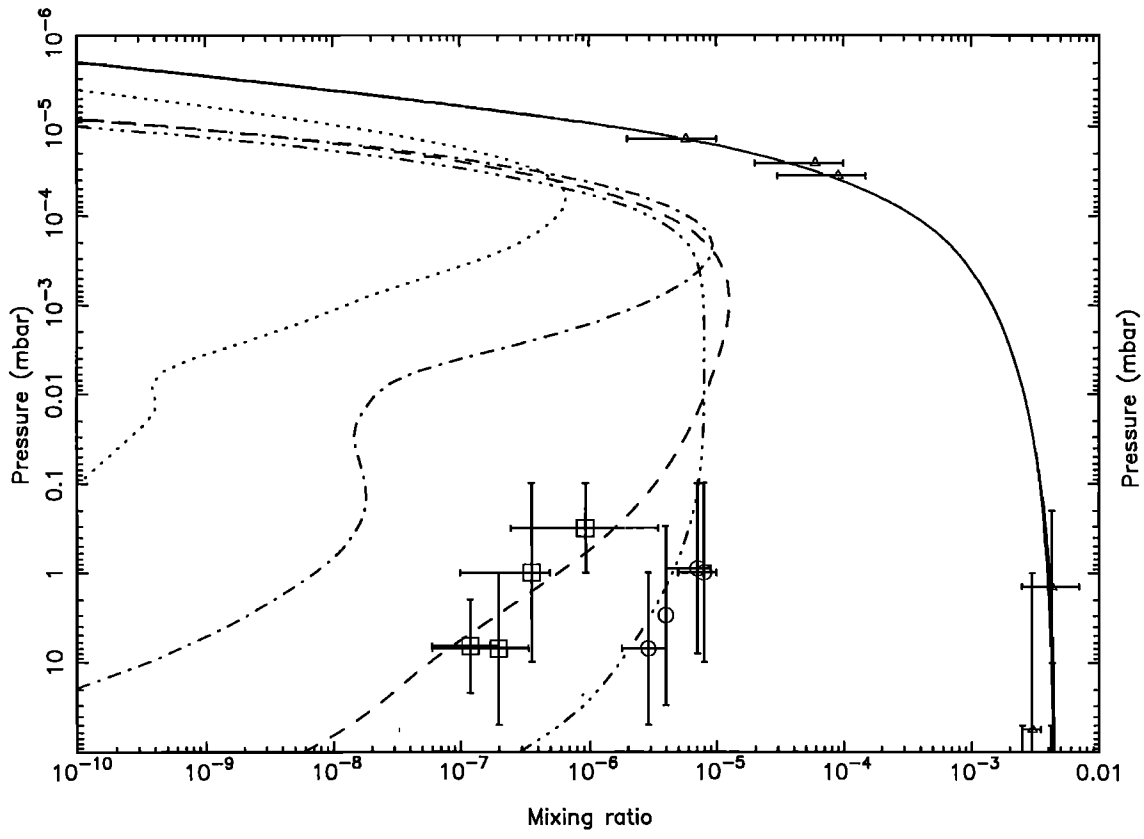

Figure 7. Same as Figure 6, but for Saturn. Voyager UVS observations: CH_4 (open triangle).

agreement with our Jupiter model. For Saturn we also compare the C_2H_2 and C_2H_6 mixing ratios from our models to the previous observations, as shown in Figure 7. On Saturn the IRIS data at midlatitudes are $f(C_2H_2) = (0.6 - 3.4) \times 10^{-7}$ and $f(C_2H_6) = (1.8 - 4.0) \times 10^{-6}$ from 5 to 100 mbar [*Courtin et al.*, 1984]. On Titan the IRIS data at midlatitudes are $f(C_2H_2) = (2.0 - 3.6) \times 10^{-6}$ and $f(C_2H_6) = (1.0 - 2.1) \times 10^{-5}$ from 1 to 10 mbar [*Coustenis et al.*, 1989; 1991]. Both Figures 7 and 10 demonstrate that our hydrocarbon profiles for Saturn and Titan compare well with both Voyager and ground-based observations. The recent observations in the stratosphere of Saturn by ISO yielded $f(C_2H_2) = 2.5 \times 10^{-7}$ and $f(C_2H_6) = 4.0 \times 10^{-6}$ from 0.3 to 30 mbar [*de Graauw et al.*, 1997]; these values also match our result.

Analysis of Voyager 2 data in the stratosphere of Uranus provides the abundance of C_2H_2 ($\approx 1 \times 10^{-8}$) and C_2H_6 ($\approx (1 - 2) \times 10^{-8}$) only at higher altitudes (above 0.1 mbar pressure level) by ultraviolet spectrometer occultation measurement [*Herbert et al.*, 1987; *Bishop et al.*, 1990]. IUE observation shows a similar result with both C_2H_2 and $C_2H_6 \approx 1 \times 10^{-8}$ above the 0.5 mbar level [*Caldwell et al.*, 1988]. Our Uranus model is in agreement with these observations at 0.1 - 0.01 mbar, as shown in Figure 8. However, hydrocarbon abundances in the lower stratosphere of Uranus still need to be verified.

The Neptune model is unusual for its eddy diffusion coefficient. Since the maximum photochemical production of C_2H_6 at the 10^{-4} mbar pressure level in our model gives an upper limit of $(1 - 2) \times 10^{-6}$ for the C_2H_6 mixing ratio at that altitude, the Voyager IRIS observation of $f(C_2H_6) = (1 - 4) \times 10^{-6}$ from 0.1 to 1.0 mbar [*Bézard et al.*, 1991] is hard to explain unless there is an extra source of C_2H_6 in the lower atmosphere or an extremely high rate of eddy mixing throughout the stratosphere [see *Romani et al.*, 1993; *Bishop et al.*, 1998]. The cold trap by C_2H_6 condensation in the tropopause region of Neptune would render extra sources ineffectual. *Romani et al.* [1993] tested different forms for K and were able to fit the IRIS observation with K profiles having relatively high values in the upper stratosphere (e.g., $K \geq 5 \times 10^7$ cm^2 s^{-1} for $p \leq 0.5$ mbar). We adopt this high eddy diffusion coefficient value from 0.5 to 10^{-4} mbar in our Neptune model and assume that the CH_4 mixing ratio is 2×10^{-4} at the tropopause. However, our models do not include the condensation calculations in the stratosphere.

We have assumed in our model that an additional source of Lyman α exists at Neptune. The enhanced Lyman α photon flux may be contributed by the diffusive scattering of solar Lyman α photons from hydrogen atoms in the interplanetary medium (IPM), as has been suggested by *Ajello* [1990], *Moses* [1991], and *Gladstone* [1993]. According to both Moses's and Gladstone's estimate, the background flux from the IPM is in the same order of magnitude as the direct Lyman α flux at the orbit of Neptune. The two Lyman α sources are assumed to be of comparable strength at the orbit of Neptune, which in our model is modeled with doubling Lyman α flux for CH_4 photodissociation. The C_2H_2 and C_2H_6 vertical mixing ratio profiles, calculated by increasing Lyman α radiation by a factor of 2, provide a good fit to the observations in Figure 9. In contrast, the direct solar Lyman α flux is obviously much larger than the diffusive Lyman α

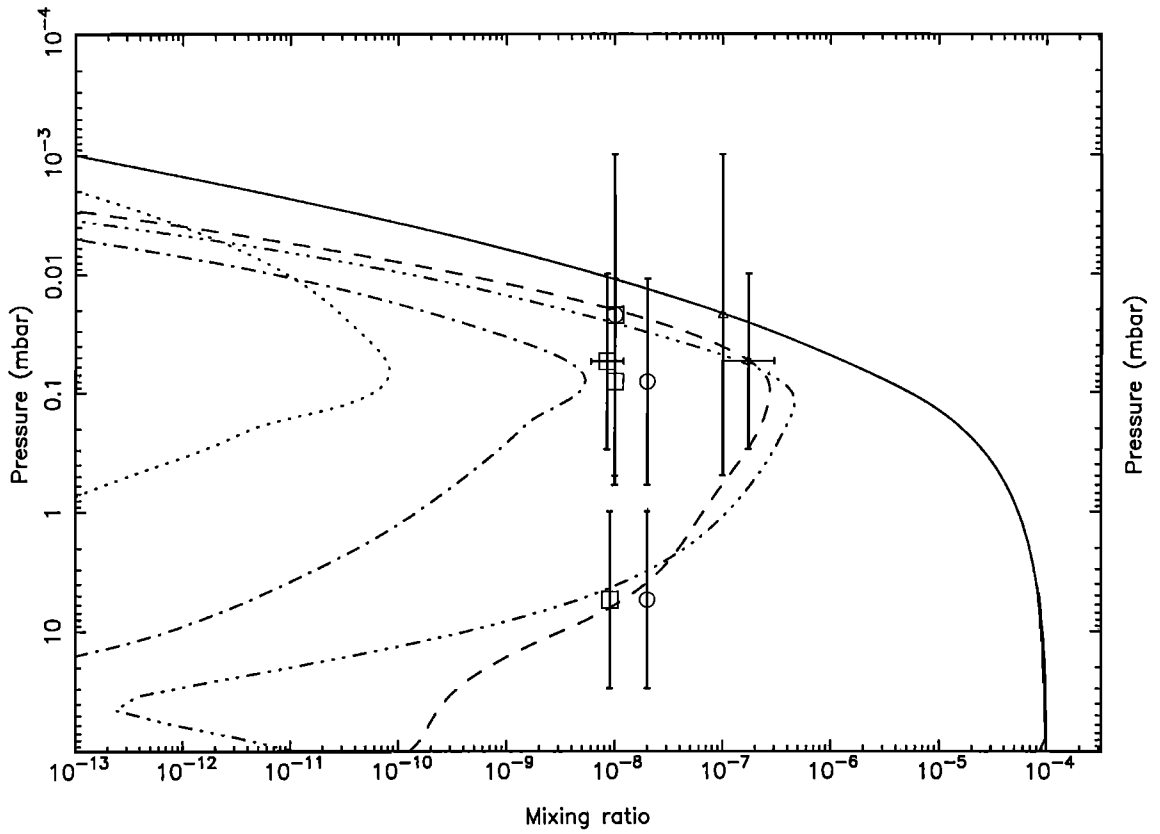

Figure 8. Same as Figure 6, but for Uranus.

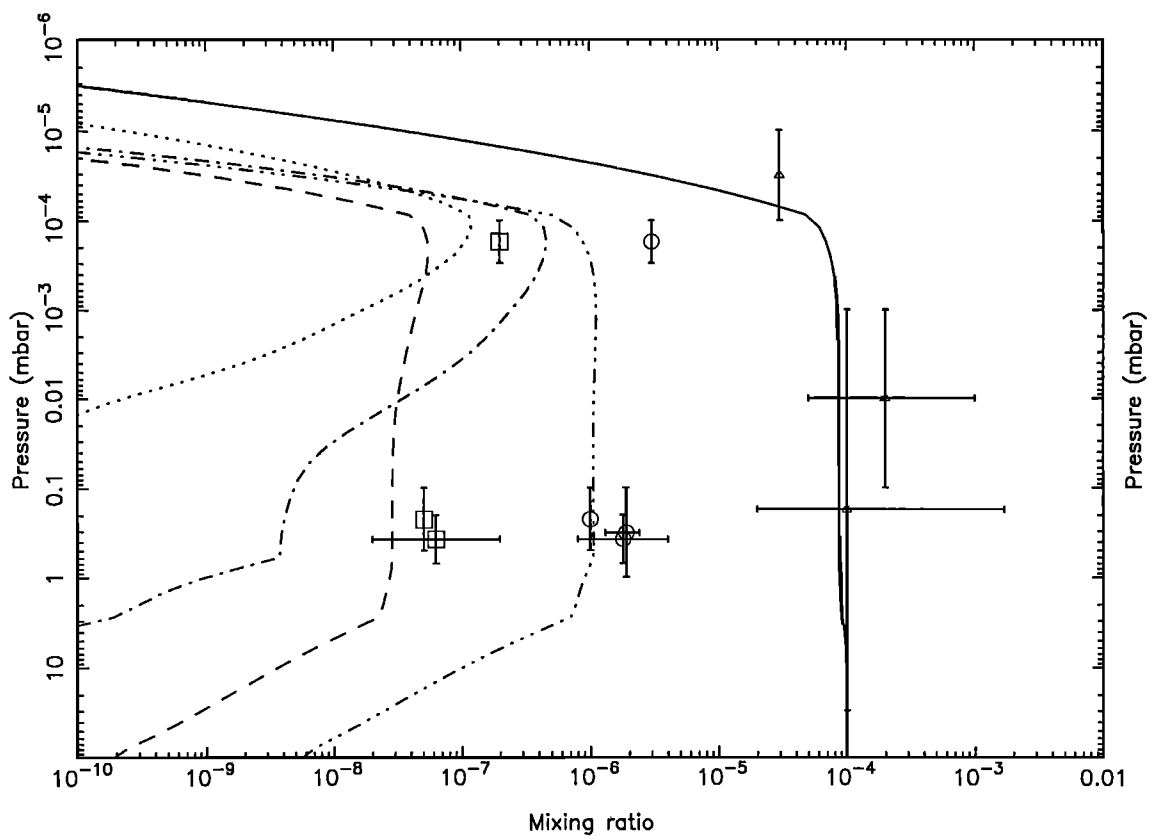

Figure 9. Same as Figure 6, but for Neptune.

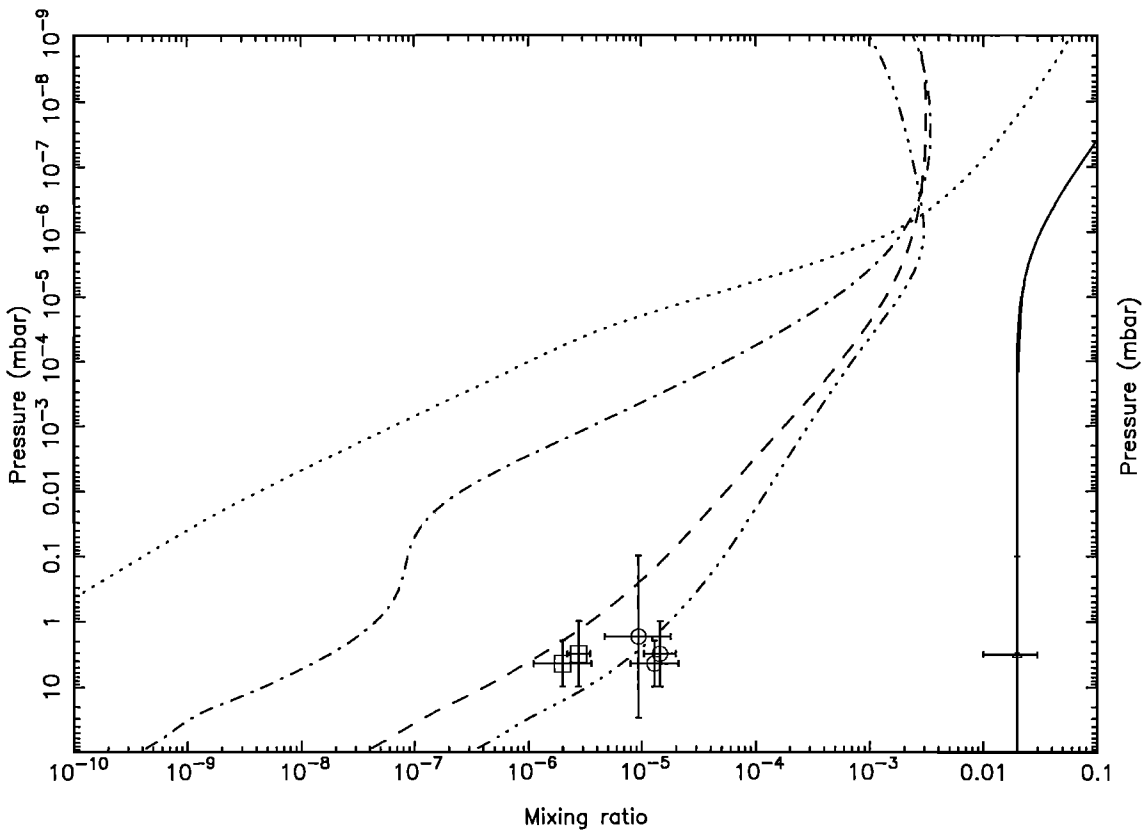

Figure 10. Same as Figure 6, but for Titan.

from IPM for Jupiter, Saturn, and Uranus. Therefore we consider only the direct solar flux in our Jupiter (Figure 6), Saturn (Figure 7), Titan, (Figure 10) and Uranus (Figure 8) models.

4. Sensitivity Tests

We test the sensitivities of our models to the temperature and eddy diffusion coefficients of Saturn and Neptune. The results are presented in Table 5. There are two types of sensitivity tests: (1) Varying temperatures by a 10 K increase or decrease at every pressure level and (2) varying eddy diffusion coefficients by a factor of 2 increase or decrease at every pressure level in the models. ISO observations and our normal model results using the "Modified Slagle" reaction rate constant are also listed in Table 5 for the purpose of comparison. We see only small changes in the CH_3 column abundances from shifting temperature profiles (± 10 K) in the stratospheres of Saturn and Neptune. This result is not surprising because our "Modified Slagle" rate constant extrapolation function (4) changes only 10% for the temperature rising or falling by 10 K near 150 K. Simultaneous temperature changes of other chemical reactions may cancel this 10% effect. However, choosing rate constant functions by "Slagle" or "MacPherson" would cause larger temperature sensitivities at low temperatures (Figure 4).

The eddy diffusion coefficient parameterizes the vertical transport of the atmospheres of the outer solar system, determining the profiles of stable molecules such as CH_4 and C_2H_6. The effects of changing the eddy diffusion coefficient are shown by the last two cases in Table 5. The CH_3 column density calculated by enhancing bulk atmospheric eddy transport by a factor of 2 in the upper atmosphere of Saturn is increased by a factor 1.5 from the standard model. In this case, the CH_4 profile is pushed upward and the optical depth unity level is moved higher, resulting in methane photolysis occurring in low-density regions where CH_3 chemical loss is less effective. Naturally, the CH_3 radical abundance decreases as we divide the bulk eddy diffusion coefficient by 2 and thus reduce the total column abundance of CH_4 above the tropopause. This effect may provide an explanation for the higher CH_3 column abundance, compared to Jupiter, in the atmosphere of Saturn, where the eddy diffusion coefficient above the 0.1 mbar pressure level is bigger than the value on Jupiter (Figure 3). The lowest CH_3 value in the atmosphere of Uranus (Table 4) is also consistent with this effect because the eddy diffusion coefficient of the stratosphere of Uranus is almost two orders of magnitude smaller than those in the other giant planets.

The Neptune model is the most sensitive to variations in the Lyman α radiation flux and to changes in chemical rate constants. We present four models for Neptune to test the sensitivity of out best fit model (Figure 9). Model 1 was carried out by assuming that all Lyman α flux comes from direct solar radiation. (Our best fit Neptune model assumes two times solar Lyman α flux at the orbit of Neptune.) Model 2 assumes that the adopted rate constant of key exchange reaction, $^1CH_2 + H_2 \rightarrow CH_3 + H$, is $k = 9.24 \times 10^{-11}$ cm^3 s^{-1} for $T < 150$ K, a value larger than the one used in our best fit model at low temperatures. Model 3 tests the recycling reaction (1), $H + CH_3 + M \rightarrow CH_4 + M$, by assuming three-body rate constant $k_0 = 2.52 \times 10^{-29}$ cm^6 s^{-1} at $T < 300$ K. This value was used by *Moses et al.* [2000a] in their Saturn model. Model 4 tests the key reaction for recycling C_2H_2, H +

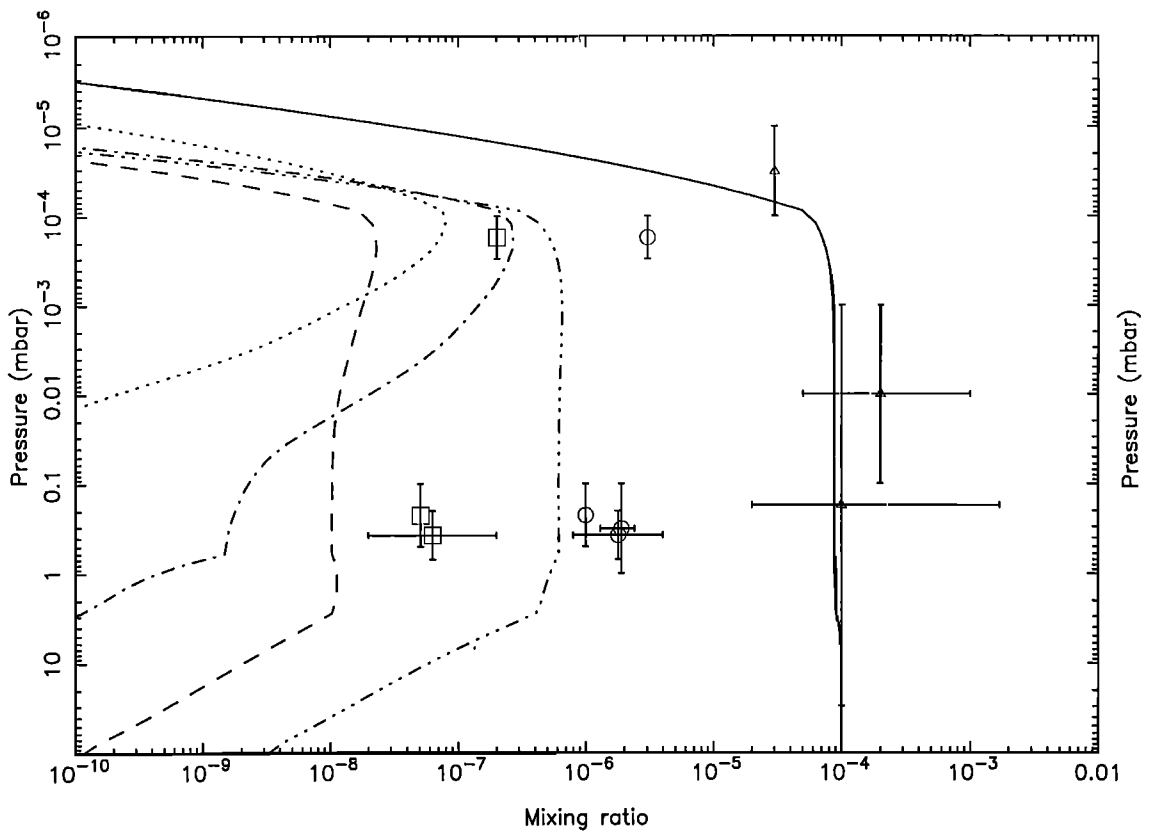

Figure 11. Model 1 for Neptune. The solar flux at Lyman α is 1/2 of our best fit model; the Lyman α comes only from direct solar radiation.

$C_2H_3 \rightarrow C_2H_2 + H_2$. The rate constant in model 4 is assumed to be 2.0×10^{-11} cm^3 s^{-1}, compared to the rate constant 7.5×10^{-11} cm^3 s^{-1} used in our best fit model (see Table 2; we should mention here that all the values in Table 2 were chosen to best fit the hydrocarbon observations in all five atmospheres of the outer solar system). The branching ratios of CH_4 photodissociation used by *Moses et al.* [2000a] (48% CH_3, 20% $^1CH_2$, 32% CH; based on *Mordaunt et al.* [1993]) have also been tested in model 5.

The resultant stable hydrocarbon vertical profiles for models 1, 2, 3, 4, and 5 on Neptune are shown in Figures 11, 12a, 13a, 14a, and 15a, respectively. The model 2, 3, 4, and 5 results for Saturn (direct solar Lyman α flux test is not needed for Saturn) are shown in Figures 12b, 13b, 14b, and 15b, respectively. The CH_3 column abundances calculated from these test models for both Saturn and Neptune are shown in Table 6.

A comparison of Figure 11 with Figure 9 provides the motivation for our consideration of an enhanced Lyman α flux in our Neptune model due to scattering in the IPM. The weak solar radiation at the distance of Neptune (~ 30 AU), three orders of magnitude less than the solar radiation received by the Earth, reduces the generation of C2 or higher hydrocarbon molecules from CH_4 dissociation. Figure 9 shows very good agreement between our model results and the observations. Using only direct solar flux, as shown in Figure 11, marginally matches the lower limit of C_2H_2 and C_2H_6 error bars of the Voyager IRIS observation. However, the CH_3 column abundance value derived from model 1 (2.1×10^{13} cm^{-2}) fits the ISO observation better than our best fit hydrocarbon model (2.8×10^{13} cm^{-2}). Since the addition of more diffusive Lyman α radiation (exceeding a factor of 2) to our Neptune model would violate the ISO CH_3 observation, our models provide an independent confirmation of the magnitude of the background IPM radiation determined by *Gladstone* [1993].

Table 6. CH_3 Column Abundances in the Upper Atmospheres of Saturn and Neptune above 10 mbar for Saturn and 0.2 mbar for Neptune Derived From Four Test Models

CH_3 Column Abundances, cm^{-2}	Saturn	Neptune
Standard model	5.1×10^{13}	2.2×10^{13}
Model 1[a]	-	1.6×10^{13}
Model 2[b]	5.2×10^{13}	2.3×10^{13}
Model 3[c]	6.6×10^{13}	2.3×10^{13}
Model 4[d]	5.0×10^{13}	2.2×10^{13}
Model 5[e]	6.5×10^{13}	3.1×10^{13}

[a]Model 1 on Neptune uses the typical solar radiation flux. Our "best fit" Neptune model doubles solar flux at Lyman α.

[b]Model 2 adopts $k = 9.24 \times 10^{-11}$ cm^3 s^{-1} ($T < 150$ K) for the temperature-independent rate constant of $^1CH_2 + H_2 \rightarrow CH_3 + H$.

[c]Model 3 adopts $k_0 = 2.52 \times 10^{-29}$ cm^6 s^{-1} for the low-pressure limit rate constant at $T < 300$ K of $H + CH_3 + M \rightarrow CH_4 + M$.

[d]Model 4 adopts $k = 2.0 \times 10^{-11}$ cm^3 s^{-1} for the temperature-independent rate constant of $H + C_2H_3 \rightarrow C_2H_2 + H_2$.

[e]Model 5 adopts CH_4 branching ratios used by *Moses et al.* [2000a]. (48% CH_3, 20% $^1CH_2$, 32% CH; based on *Mordaunt et al.* [1993]).

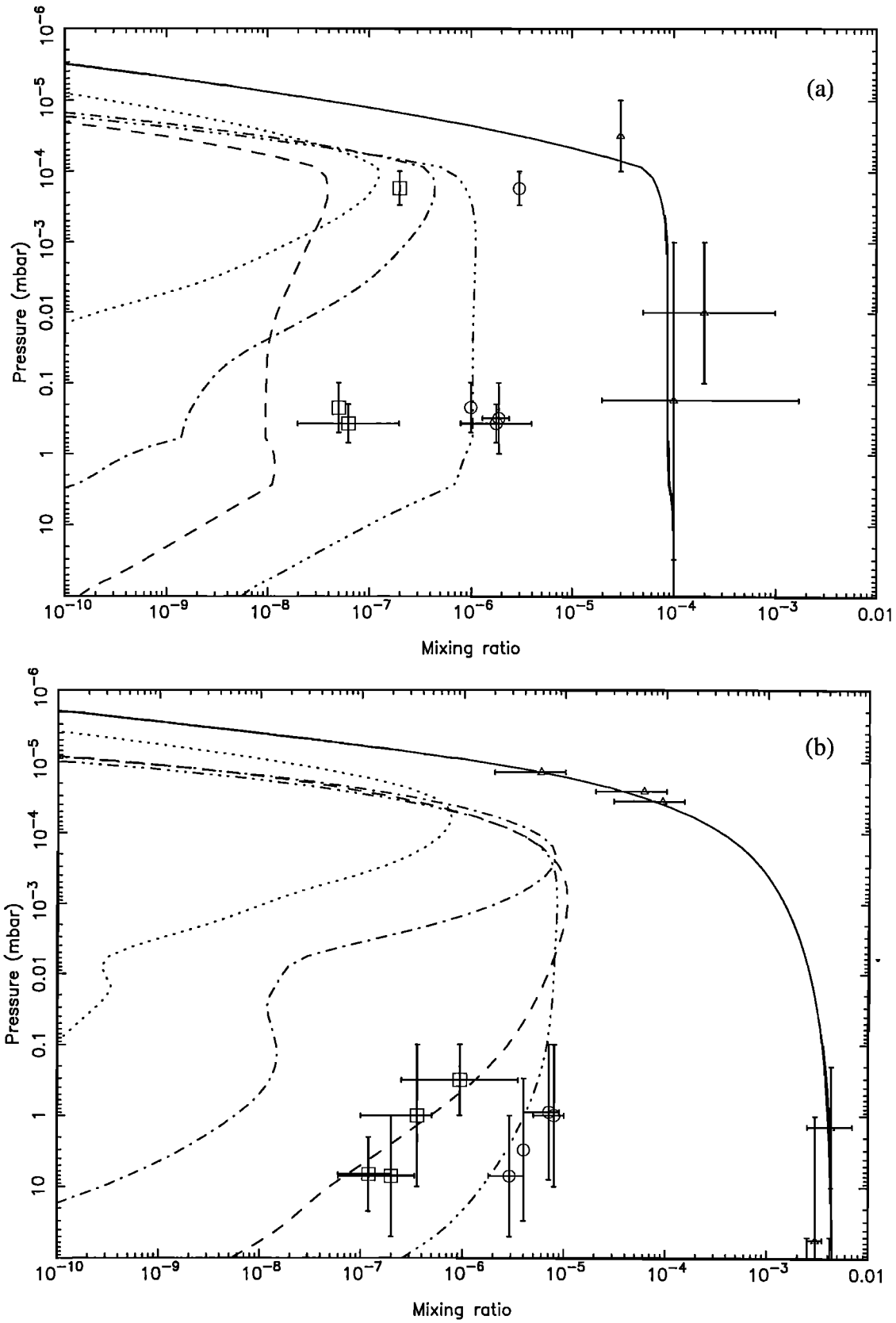

Figure 12. Model 2 for (a) Neptune, and (b) Saturn. The rate constant of $^1CH_2 + H_2 \rightarrow CH_3 + H$ is $k = 9.24 \times 10^{-11}$ cm^3 s^{-1} for all temperatures.

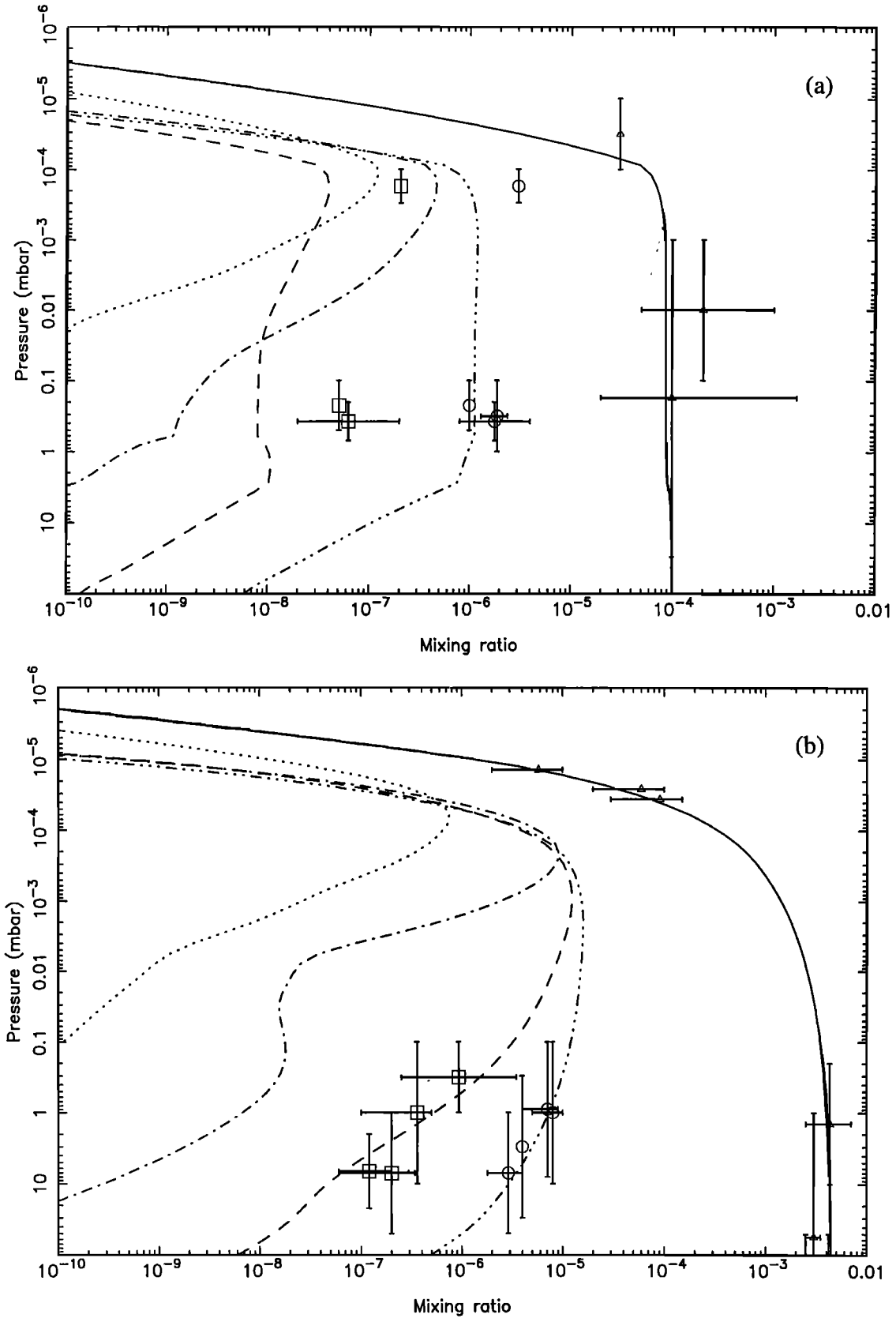

Figure 13. Model 3 for (a) Neptune, and (b) Saturn. The rate constant of H + CH_3 + M → CH_4 + M is k_0 = 2.52×10^{-29} cm^6 s^{-1} ($T < 300$ K).

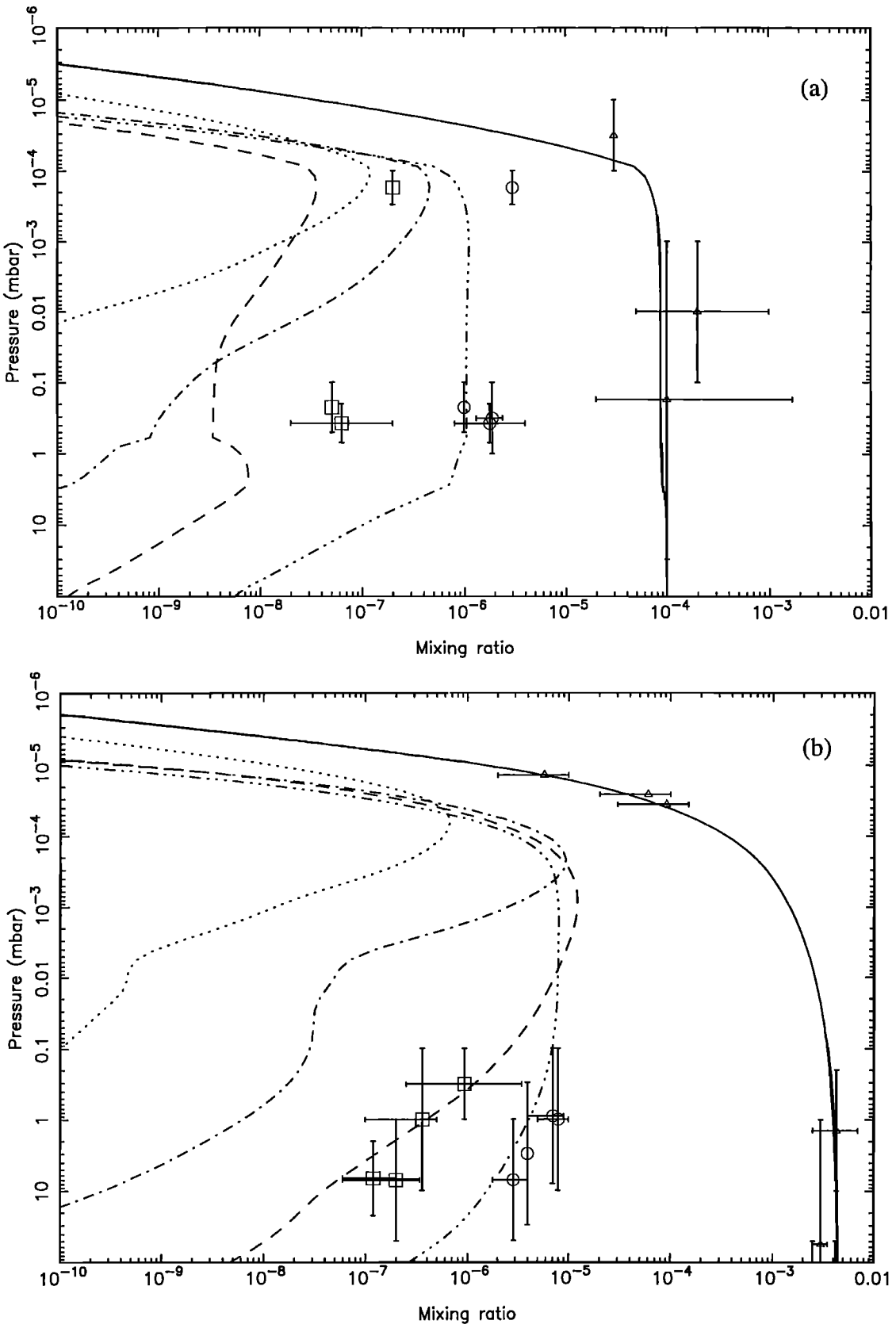

Figure 14. Model 4 for (a) Neptune, and (b) Saturn. The rate constant of $H + C_2H_3 \rightarrow C_2H_2 + H_2$ is $k = 2.0 \times 10^{-11}$ cm^3 s^{-1}.

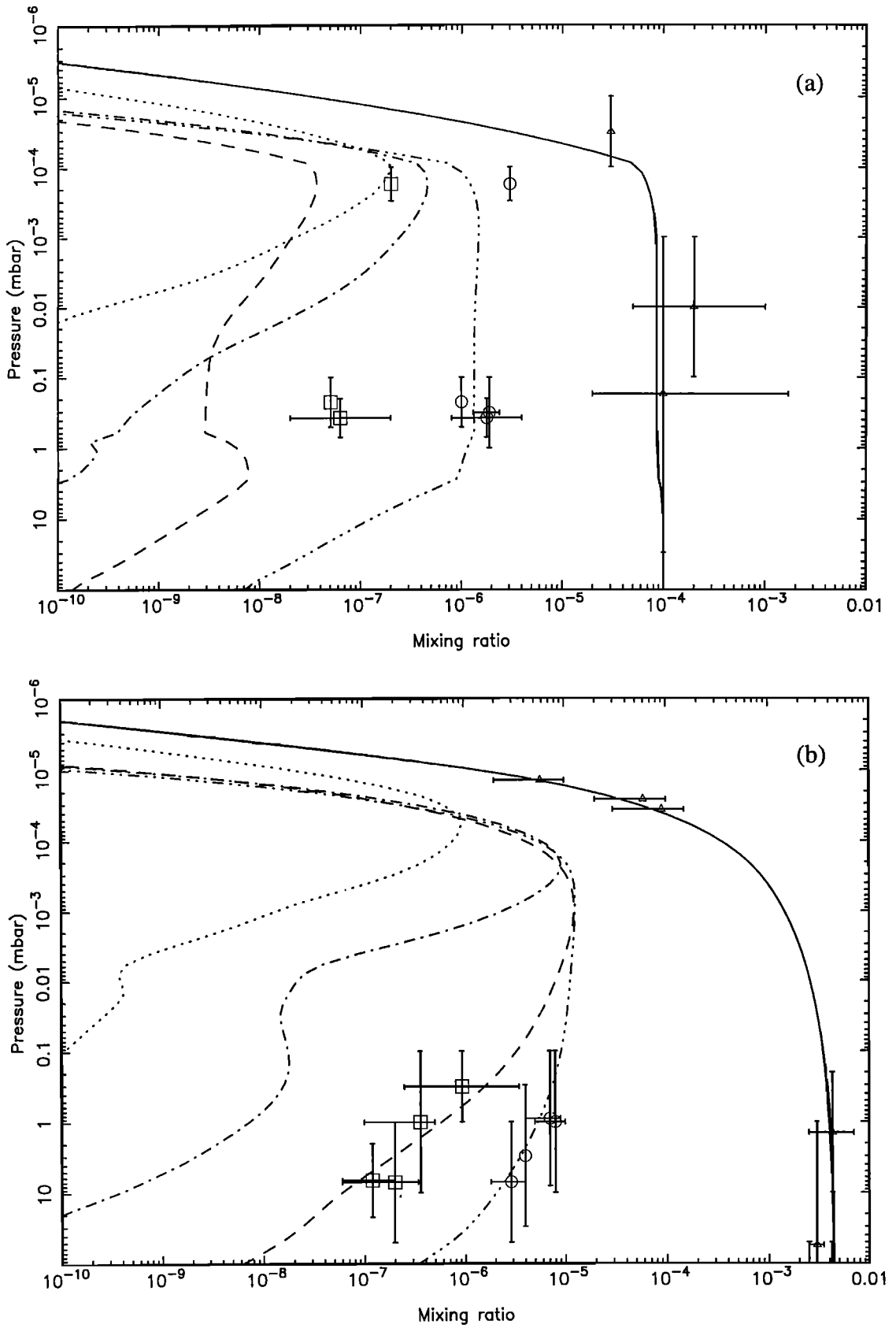

Figure 15. Model 5 for (a) Neptune, and (b) Saturn. The CH_4 branching ratios are 48% CH_3, 20% $^1CH_2$, 32% CH.

Models 2, 3, and 4 provide the chemical sensitivity studies for our best fit model. Three sensitivity tests of the key reactions listed in Table 2 affecting stable hydrocarbon products for Neptune are shown in Figures 12a, 13a, and 14a, and for Saturn are shown in Figures 12b, 13b, and 14b. It is obvious that these changed rate constants are more sensitive in the case of Neptune than in the case of Saturn. For example, changing the rate constant of the reaction $^1CH_2 + H_2 \rightarrow CH_3 + H$ from 9.24×10^{-11} cm^3 s^{-1} to 7.0×10^{-11} cm^3 s^{-1} for $T < 150$ K in the Saturn model provides only a ~10% decrease of C_2H_2 and C_2H_6 mixing ratios at 0.1 mbar. On the other hand, it gives a factor of 3 less C_2H_2 in the Neptune model at the same level. Changing only single key rate constants does not violate the model fit to C_2H_2 and C_2H_6 observational values on Saturn, as is shown in Figures 12b, 13b, and 14b. However, such changes affect Neptune more significantly, especially for the C_2H_2 mixing ratio profile (see Figures 12a, 13a, and 14a). Because we use the same chemical model in the five atmospheres, each estimated kinetic value should be constrained to observations on all of these planets and the satellite. Therefore the chemical rate constants adjusted in our models are more acceptable than those derived only from a single atmospheric model. We notice that these newly estimated rate constants have larger influences on the C_2H_2 mixing ratio in the lower stratosphere of Neptune than the C_2H_6 abundance. In model 2, as shown in Figure 12a, increasing the reaction rate of $^1CH_2 + H_2 \rightarrow CH_3 + H$ provides significant depletion of C_2H_2 in the lower stratosphere of Neptune. In fact, the C_2H_2 mixing ratio fails to fit the lower limit of the Voyager IRIS error bar for an assumed increased rate constant of $k = 9.24 \times 10^{-11}$ cm^3 s^{-1}. This significant effect is not so obvious in the Jupiter or Saturn models.

Models 3 and 4, as shown in Figures 13a and 14a, respectively, demonstrate the sensitivity of the Neptune model to the reactions $H + CH_3 + M \rightarrow CH_4 + M$ and $H + C_2H_3 \rightarrow C_2H_2 + H_2$. Since these reactions still lack reliable experimental rate constants at low temperatures, our models, especially the Neptune model, may provide a constraint on the theoretical estimates of chemical kinetics.

Model 5 examines the influence of CH_4 branching ratios on our hydrocarbon models. The major difference between the *Slanger and Black* [1982] values and the *Mordaunt et al.* [1993] values is that the former lacks the $CH_4 \rightarrow CH_3 + H$ channel, and this channel is the major pathway for the other case. We replace the branching ratios by those adopted in *Moses et al.*'s [2000a] model in our sensitivity test model 5. According to Figure 15b and the last row in Table 6, there are only slight changes between the two sets of branching ratios on Saturn for C2 hydrocarbon and CH_3 column abundances. However, there is a significant decrease for C_2H_2 by adopting Mordaunt et al. branching ratios for Neptune (Figure 15a).

5. Conclusions

Generalized one-dimensional photochemical models using a single chemical reaction set have been applied to the atmospheres of the giant planets and Titan for the first time. We adopt the most complete and recent updated set of hydrocarbon photochemical reactions and cross sections from *Moses et al.* [2000a], except that we test and modify some rate constants and methane photolysis branching ratios. The key reactions that we estimate are $CH_3 + CH_3 + M \rightarrow C_2H_6 + M$, $H + CH_3 + M \rightarrow CH_4 + M$, and $H + C_2H_3 \rightarrow C_2H_2 + H_2$. In this article we suggest a modified formula for the rate coefficient of the recombination reaction $CH_3 + CH_3 + M \rightarrow C_2H_6 + M$ at low temperatures, and we also evaluate the rate constants of other key reactions. We calculate the mixing ratio of hydrocarbon species at each altitude level and determine the total column concentrations of methyl radicals in the stratospheres of Jupiter, Saturn, Uranus, Neptune and Titan. All models are distinguished by their physical properties, such as distance to the Sun and gravity, and their atmospheric characteristics, such as temperature profile and vertical eddy mixing coefficients. The Lyman α flux enhancement at the Neptune's orbit has also been considered.

Our models provide reasonable results compared to the ISO/SWS observations of CH_3 on both Saturn and Neptune. Our modified rate constant formula for the reaction $CH_3 + CH_3 + M \rightarrow C_2H_6 + M$ at low temperatures, incorporated with other estimated rate constants (Table 2), also provides good agreement to observations of the stable hydrocarbon species. However, reliable experimental low-temperature kinetics data for most of the reactions listed in Table 2 are still lacking. This limitation should provide strong motivation for future laboratory studies. Our prediction for low CH_3 concentrations in the upper stratosphere of Uranus, and a high CH_3 abundance on Titan, can be checked by future observations.

Acknowledgments. We thank W. DeMore and K. Bayes for valuable theoretical chemical rate constant estimates. We also thank M. Allen, M. Gerstell, and two anonymous referees for helpful comments. This research is supported by NASA grant NAG5-6263 to the California Institute of Technology.

References

Ajello, J. M., Solar minimum Lyman α sky background observations from Pioneer Venus orbiter ultraviolet spectrometer: Solar wind latitude variation, *J. Geophys. Res., 95*, 14,855-14,861, 1990.

Allen, M., Chemical kinetics: A planetary review, *First International Conference on Laboratory Research for Planetary Atmospheres, NASA Conf. Publ., CP-3077*, 443-450, 1989.

Ashfold, M. N. R., I. R. Lambert, D. H. Mordaunt, G. P. Morley, and C. M. Western, Photofragment translational spectroscopy, *J. Phys. Chem., 96*, 2938-2949, 1992.

Atreya, S. K., S. G. Edgington, Th. Encrenaz, and H. Feuchtgruber, Observations of C_2H_2 on Uranus and CH_3 on Saturn: Implications for atmospheric vertical mixing in the Voyager and ISO epochs, and a call for relevant laboratory measurements; *The Universe as Seen by ISO, Eur. Space Agency Spec. Publ., ESA SP-427*, 1998.

Baulch, D. L., et al., Warnatz, Evaluated kinetic data for combustion modeling, *J. Phys. Chem. Ref. Data, 21*, 411-734, 1992.

Bézard, B., P. N. Romani, and B. J. Conrath, Hydrocarbons in Neptune stratosphere from Voyager infrared observations, *J. Geophys. Res., 96*, 18,961-18,975, 1991.

Bézard, B., H. Feuchtgruber, and Th. Encrenaz, Detection of methyl radicals (CH_3) on Saturn, *Astron. Astrophys., 334*, L41-L44, 1998.

Bézard, B., P. N. Romani, H. Feuchtgruber, and Th. Encrenaz, Detection of the methyl radical on Neptune, *Astrophys. J., 515*, 868-872, 1999.

Bishop, J., S. K. Atreya, F. Herbert, and P. N. Romani, Reanalysis of Voyager 2 UVS occultations at Uranus: Hydrocarbon mixing ratios in the equatorial stratosphere, *Icarus, 88*, 448-464, 1990.

Bishop, J., P. N. Romani, and S. K. Atreya, Voyager 2 ultraviolet spectrometer solar occultations at Neptune: Photochemical modeling of the 125-165 nm lightcurves, *Planet. Space Sci., 46*, 1-20, 1998.

Broadfoot, A. L. et al., Ultraviolet spectrometer observations of Neptune and Triton, *Science, 246*, 1459-1466, 1989.

Brouard, M., M. T. MacPherson, and M. J. Pilling, Experimental and RRKM modeling study of the CH_3 + H and CH_3 + D reactions, *J. Phys. Chem., 93*, 4047-4059, 1989.

Caldwell, J., R. Wagner, and K. H. Fricke, Observations of Neptune and Uranus below 2000 A with the IUE, *Icarus, 74*, 133-140, 1988.

Courtin, R., D. Gautier, A. Marten, B. Bézard, and R. Hanel, The composition of Saturn's atmosphere at northern temperate latitudes from Voyager IRIS spectra: NH_3, PH_3, C_2H_2, C_2H_6, CH_3D, CH_4, and the Saturnian D/H isotopic ratio, *Astrophys. J., 287*, 899-916, 1984.

Coustenis, A., B. Bézard, and D. Gautier, Titan's atmosphere from Voyager infrared observations, 1, The gas-composition of Titan's equatorial region, *Icarus, 80*, 54-76, 1989.

Coustenis, A., B. Bézard, D. Gautier, A. Marten, and R. Samuelson, Titan's atmosphere from Voyager infrared observations, 3, Vertical distributions of hydrocarbons and nitriles near Titan's north pole, *Icarus, 89*, 152-167, 1991.

de Graauw, T., et al., First results of ISO-SWS observations of Saturn: Detection of CO_2, CH_3C_2H, C_4H_2 and tropospheric H_2O, *Astron. Astrophys., 321*, L13-L16, 1997.

Du, H., J. P. Hessler, and P. J. Ogren, Recombination of methyl radicals, 1, New Data between 1175 and 1750 K in the falloff region, *J. Phys. Chem., 100*, 974-983, 1996.

Forst, W., Microcanonical variational theory of radical recombination by inversion of interpolated partition function, with examples: CH_3 + H, CH_3 + CH_3, *J. Phys. Chem., 95*, 3612-3620, 1991.

Gladstone, G. R., Photochemistry in the primitive solar nebula, *Science, 261*, 1058, 1993.

Gladstone, G. R., M. Allen, and Y. L. Yung, Hydrocarbon photochemistry in the atmosphere of Jupiter, *Icarus, 119*, 1-52, 1996.

Heck, A. J. R., R. N. Zare, and D. W. Chandler, Photofragment imaging of methane, *J. Chem. Phys., 104*, 4019-4030, 1996.

Heinemann, P., R. Hofmann-Sievert, and K. Hoyermann, Direct study of the reactions of vinyl radicals with hydrogen and oxygen atoms, *Symp. Int. Combust., 21st*, 5-873, 1986.

Herbert, F., B. R. Sandel, and R. V. Yelle, The upper atmosphere of Uranus–EUV occultations observed by Voyager 2, *J. Geophys. Res., 92*, 15,093-15,109, 1987.

Hole, K. J., and M. F. R. Mulcahy, The photolysis of biacetyl and the third-body effect on the combination of methyl radicals, *J. Phys. Chem., 73*, 177-185, 1969.

Klippenstein, J. K., and L. B. Harding, A direct transition state theory based study of methyl radical recombination kinetics, *J. Phys. Chem., 103*, 9388-9398, 1999.

Kostiuk, T. P., N. Romani, and F. Espenak, Stratospheric ethane on Neptune: Comparison of groundbased and Voyager IRIS retrievals, *Icarus, 99*, 353-362, 1992.

Langford, A. O., H. Petek, and C. B. Moore, Collisional removal of $CH_2(^1A_1)$: Absolute rate constants for atomic and molecular collisional partners at 295 K, *J. Chem. Phys., 78*, 6650-6659, 1983.

Lara, L. M., E. Lellouch, J. J. LopezMoreno, and R. Rodrigo, Vertical distribution of Titan's atmospheric neutral constituents, *J. Geophys. Res., 101*, 23,261-23,283, 1996.

Laufer, A. H., E. P. Gardner, T. L. Kwok, and Y. L. Yung, Computations and estimates of rate coefficients for hydrocarbon reactions of interest to the atmospheres of the outer solar system, *Icarus, 56*, 560-567, 1983.

Lindal, G. F., D. N. Sweetnam, and V. R. Eshleman, The atmosphere of Saturn: An analysis of the Voyager radio occultation measurements, *Astron. J., 90*, 1136-1146, 1985.

Lindal, G. F., The atmosphere of Neptune: An analysis of radio occultation data acquired with Voyager 2, *Astron. J., 103*, 967-982, 1992.

MacPherson, M. T., M. J. Pilling, and M. J. C. Smith, The pressure and temperature dependence of the rate constant for methyl radical recombination over the temperature range 296-577 K, *Chem. Phys. Lett., 94*, 430-433, 1983.

MacPherson, M. T., M. J. Pilling, and M. J. C. Smith, Determination of the absorption cross section for CH_3 at 216.36 nm and the absolute rate constant for methyl radical recombination over the temperature range 296-577 K, *J. Phys. Chem., 89*, 2268-2274, 1985.

Monks, P. S., F. L. Nesbitt, W. A. Payne, M. Scanlon, and L. J. Stief, Absolute rate constant and product branching ratios for the reaction between H and C_2H_3 at T=213 and 298 K, *J. Phys. Chem., 99*, 17,151-17,159, 1995.

Mordaunt, D. H., I. R. Lambert, G. P. Morley, M. N. R. Ashford, R. N. Dixon, and C. M. Western, Primary product channels in the photodissociation of methane at 121.6 nm, *J. Chem. Phys., 98*, 2054-2065, 1993.

Moses, J. I., Photochemistry and aerosol formation in Neptune's atmosphere, Ph.D. thesis, Calif. Inst. of Technol., Pasadena, 1991.

Moses, J. I., B. Bézard, E. Lellouch, G. R. Gladstone, H. Feuchtgruber, and M. Allen, Photochemistry of the upper atmosphere of Saturn, I, Hydrocarbon chemistry and comparisons with ISO observations, *Icarus, 143*, 244-298, 2000a.

Moses, J. I., B. Bézard, E. Lellouch, G. R. Gladstone, H. Feuchtgruber, and M. Allen, Photochemistry of the upper atmosphere of Saturn, II, Effects of an external oxygen influx, *Icarus*, in press, 2000b.

Pilling M. J., and J. A. Robertson, Flash photolysis of ketene, photolysis mechanism and rate constants for singlet and triplet methylene, *J. Chem. Soc. Faraday Trans. 1, 73*, 968-984, 1977.

Robertson, S. H., M. J. Pilling, D. L. Baulch, and N. J. B. Green, Fitting of pressure-dependent kinetic rate data by master equation/inverse Laplace transform analysis, *J. Phys. Chem., 99*, 13,452-13,460, 1995.

Romani, P. N., Recent rate constant and product measurements of the reactions C_2H_3 + H_2 and C_2H_3 + H – Importance for photochemical modeling of hydrocarbons on Jupiter, *Icarus, 122*, 233-241, 1996.

Romani, P. N., J. Bishop, B. Bézard, and S. K. Atreya, Methane photochemistry on Neptune: Ethane and acetylene mixing ratios and haze production, *Icarus, 106*, 442-463, 1993.

Sada, P. V., G. L. Bjoraker, D. E. Jennings, G. H. McCabe, and P. N. Romani, Observations of CH_4, C_2H_6, and C_2H_2 in the stratosphere of Jupiter, *Icarus, 136*, 192-201, 1998.

Sillesen, A., E. Ratajczak, and P. Pagsberg, Kinetics of the reactions H + C_2H_4 → C_2H_5, H + C_2H_5 → $2CH_3$, and CH_3 + C_2H_5 → Products studied by pulse radiolysis combined with infrared diode laser spectroscopy, *Chem. Phys. Lett., 201*, 171-177, 1993.

Slagle, I. R., D. Gutman, J. W. Davies, and M. J. Pilling, Study of the recombination reaction CH_3 + CH_3 → C_2H_6, 1, Experiment, *J. Phys. Chem., 92*, 2455-2462, 1988.

Slanger, T. G., and G. Black, Photodissociation channels of 1216 A for H_2O, NH_3, and CH_4, *J. Chem. Phys., 77*, 2432-2437, 1982.

Smith, N. S., and F. Raulin, Modeling of methane photolysis in the reducing atmospheres of the outer solar system, *J. Geophys. Res., 104*, 1873-1876, 1999.

Strobel, D. F., The photochemistry of methane in the Jovian atmosphere, *J. Atmos. Sci., 26*, 906-911, 1973.

Strobel, D. F., Aeronomy of the major planets: Photochemistry of ammonia and hydrocarbons, *Rev. Geophys., 13*, 372-382, 1975.

Summers, M. E., and D. F. Strobel, Photochemistry of the atmosphere of Uranus, *Astrophys. J., 346*, 495-508, 1989.

Toublanc, D., J. P. Parisot, J. Brillet, D. Gautier, F. Raulin, and C. P. McKay, Photochemical modeling of Titan's atmosphere, *Icarus, 113*, 2-26, 1995.

Troe, J., Theory of thermal unimolecular reactions at low pressure, I, Solutions of the master equation, *J. Chem. Phys., 66*, 4745-4757, 1977a.

Troe, J., Theory of thermal unimolecular reactions at low pressure, II, Strong collision rate constants, applications, *J. Chem. Phys., 66*, 4758-4775, 1977b.

Van den Bergh, H. E., The recombination of methyl radicals in the low pressure limit, *Chem. Phys. Lett., 43*, 201-204, 1976.

Wagner, A. F., and D. M. Wardlaw, Study of the recombination reaction CH_3 + CH_3 → C_2H_6, 2, Theory, *J. Phys. Chem., 92*, 2462-2471, 1988.

Yung, Y. L., and W. B. DeMore, *Photochemistry of Planetary Atmospheres*, Oxford Univ. Press, New York, 1999.

Yung, Y. L., M. Allen, and J. P. Pinto, Photochemistry of the atmosphere of Titan: Comparison between model and observations, *Astrophys. J. Suppl. Ser., 55*, 465-506, 1984.

A. Y. T. Lee, and Y. L. Yung, Division of Geological and Planetary Sciences, California Institute of Technology, Mail Stop 150-21, Pasadena, CA 91125. (ytl@gps.caltech.edu and yly@gps.caltech.edu)

J. Moses, Lunar and Planetary Institute, 3600 Bay Area Boulvard, Houston, TX 77057-1113. (moses@lpi.usra.edu)

(Received September 20, 1999; revised April 6, 2000; accepted April 11, 2000.)